X-531-65-403

NASA TM X-55382

THE GODDARD RANGE AND RANGE RATE TRACKING SYSTEM: CONCEPT, DESIGN AND PERFORMANCE

BY

G. C. KRONMILLER, JR.

E. J. BAGHDADY

OCTOBER 1965

NASA — GODDARD SPACE FLIGHT CENTER

GREENBELT, MARYLAND

THE GODDARD RANGE AND RANGE RATE TRACKING SYSTEM: CONCEPT, DESIGN AND PERFORMANCE

G. C. Kronmiller, Jr.,* and E. J. Baghdady**

ABSTRACT

This paper is concerned with the concept, evolution and performance analysis of a high-accuracy, near-earth and cislunar cooperative target tracking system, known as the Goddard Range and Range Rate System.

This system combines the advantages of harmonic (or sidetone) and pseudo-random coded ranging signals in a highly effective and versatile manner, operable either as an all-harmonic system in near-earth orbital tracking or as a hybrid system for tracking more distant spacecraft. The system also combines the utilization of the two types of signals in a very attractive technique for speeding up the process of acquiring the ambiguity-resolving code component in tracking spacecraft at cislunar and translunar distances.

The theoretical analysis of system performance and errors is followed by a summary of performance data gathered to date by operating GRARR systems on a number of NASA missions.

---

* Goddard Space Flight Center, National Aeronautics and Space Administration, Greenbelt, Md.

** ADCOM, Inc., Cambridge, Mass.

THE GODDARD RANGE AND RANGE RATE TRACKING SYSTEM: CONCEPT, DESIGN AND PERFORMANCE

George C. Kronmiller, Jr.
NASA/Goddard Space Flight Center,
Greenbelt, Maryland

Elie J. Baghdady
ADCOM, Inc.
Cambridge, Massachusetts

1. Introduction

This paper is concerned with the concept, evolution and performance analysis of a high-accuracy, near-earth and cislunar cooperative target tracking system, known as the Goddard Range and Range Rate System.

Until recently, the need for tracking existed only in connection with fairly large vehicles such as aircraft and missiles at relatively close ranges. Conventional high-power radar systems as well as angle measuring interferometer systems were developed for this purpose and performed adequately. However, with the advent of the artificial satellite as a tool for furthering research in space, the need for precise determination and prediction of positions of very small spacecraft at large distances (100 miles to interplanetary distances) became pressing, calling for new techniques and systems to perform the necessary tracking functions.

Several systems for tracking spacecraft have evolved within the last few years. Notable among these is the world-wide Minitrack System and the Goddard Range and Range Rate (henceforth abbreviated GRARR) System. Minitrack is a radio interferometer that measures the angle between the observer's reference plane and the line from a reference point in the plane to the satellite. This system operates at 136 mc (earlier, 108 mc) and uses a light-weight, low-power beacon from the spacecraft which can also serve

as a telemetry carrier. Thus the added spacecraft system requirements for tracking are a bare minimum. Minitrack has been extremely successful and to this day is the "work horse" of NASA's Space Tracking and Data Acquisition Network (STADAN).

When Minitrack was developed, spacecraft missions were planned for low circular orbits. Then, as spacecraft technology advanced, the interest shifted to highly elliptical orbits and space probes. An angle measuring system suffers under these conditions because of the great distances the spacecraft can move with little change in angle, especially near apogee for an elliptical orbit. New techniques were obviously needed. The GRARR system, developed to fill this need, represents a significant advance over the Minitrack System.

The GRARR system evolved as the result of recourse to the examination of all considerations of fundamental significance. A study of the possible parameters one could measure led to the choice of range, or radial distance, and range rate, or radial velocity. The choice of using a steerable antenna with the system would also provide a fairly accurate angle measurement. Several other factors then had to be chosen: the type of signal structure to use for making the range measurement, the implementation of the doppler system, the r-f carrier frequency, the modulation and demodulation processes, etc.

It was fairly obvious that the system would need some form of a transponder in the spacecraft. Spacecraft limitations placed a real restriction on the size, weight and power consumption of the system transponder. This factor was the predominant one in selecting the type of signal structure to be used in making the range measurement. The tracking signal would have to require a minimum of bandwidth and lend itself favorably to detection on the ground. The ideal signal for this application is a sine wave.

The implementation of the doppler system proved more of a problem. A means was required for eliminating the effects of spacecraft oscillator instabilities that would render the range-rate measurement useless. A second consideration was the desirability of making simultaneous measurements from three stations for a trilateration that would produce a complete orbit solution from one observation interval. This would be useful for evaluating injection into orbit or the second burning of the launch vehicle. Both of these problems were solved by a transponder technique that translates the received carrier to a low i-f frequency (around 1 to 3 mc) and then modulates this whole spectrum on the new downlink carrier.

The choice of r-f carrier was complicated by the various mission requirements. A large number of missions was being planned around small spacecraft operating in the VHF region and large spacecraft were being planned that required increasingly precise measurements. A study of ionospheric errors showed that range measurement with signals in the VHF region was affected to the extent of several hundred meters, while above 1 kmc these errors were negligible. The solution to this dilemma was to build two separate systems, one at VHF and one at S-Band.

After the preceding preliminary decisions, the details of system design remained to be worked out. Basic considerations in signal design and evaluation of systems using various types of signal designs in the light of the requirements of near-earth orbits and trajectories with high dynamics led to the adoption of a signal structure consisting of a set of "sidetones" for precision measurements and ambiguity resolution to moderate distances, supplemented by an ambiguity resolving code for resolving ambiguities to lunar distances and beyond. The basic considerations and preliminary evaluations and comparisons are presented in Section 2.

The basic system for S-Band operation, to be described in Section 3, consists of a 100 kc sidetone for the precise measurement, additional sidetones down to 8 cps and a digital code for ambiguity resolution. The VHF system, because of bandwidth restrictions, uses a 20-kc sidetone for the precise measurement. Measurement of phase with a precision of 1 percent provides range measurement with a precision of *15 meters with a 100-kc tone, and ±75 meters with a 20-kc tone. Range rate can be measured to 0.1 m/sec in the S-Band system and 1.0 m/sec in the VHF system. A system design and performance analysis is presented in Section 4.

In order to provide good world-wide coverage, system station locations were chosen at Rosman, N. C.; Carnarvon, Australia, Tananarive, Madagascar; Fairbanks, Alaska; and Santiago, Chile. The first three systems in their present form use sidetones exclusively, the last two use sidetones supplemented by an ambiguity resolving code.

The system has thus far been successfully used to track four spacecraft: IMPs A, B and C on VHF and OGO-A on S-Band. The results will be discussed in Section 5. The fundamental techniques of this system have also been successfully employed in tracking communication satellites. Special systems in which the range tones are transmitted over a communication channel have been built for the SYNCOM and for the Applications Technological Spacecraft Programs.

A most interesting current program, called GEOS, consists of a tracking experiment in which the spacecraft will be tracked by several means, using laser beams, cameras, interferometers, pure doppler, and radio (transponder). This will provide a unique opportunity to compare data from all of these various systems.

2. Preliminary Considerations[1, 2]

2.1 Fundamental Characteristics of Ranging Signals

In a general sense, the process of ranging to a cooperative transponder consists of the repeated transmission of a signal pattern, or "event," to the transponder and back to the source, and measuring the round-trip

transit time. The round-trip transit time is evidently the distance on the time scale through which one would have to shift the originally transmitted "event" in order to make it coincide exactly (i. e., in phase) with its returned replica. If the repetition period of the transmitted "event" is longer than the expected round-trip transit time, then the output of the "event" generator will line up in exact phase with its returned replica only once as we slide it in time through a distance that equals the round-trip transit time.

The operation performed to establish the above alignment of signal and return consists of cross-correlating time shifted replicas of the original output of the "event" generator with the returned signal plus noise. Since the exact time delay, ρ, between the transmitted and received signals is not known in advance, the process is carried out by a trial-and-error procedure. Certain delays, τ, are tried, and the cross-correlation values for each delay are computed. The signal contribution to the cross-correlation will be $R_{ss}(\tau) = R_s(\rho - \tau)$. The noise corrupting the returned signal contributes a term $R_{sn}(\tau)$ given by the cross-correlation of this noise with the local replica of the signal. For random noise, $R_{sn}(\tau)$ is, in general, independent of τ. The time shift from the original reference that yields the absolute maximum of the autocorrelation function of the signal is precisely the desired round-trip transit time. If the autocorrelation function $R_s(\tau)$ is relatively flat, i. e., $R_s(\tau) \approx R_s(0)$ for a considerable range of τ, a small amount of noise can cause a considerable uncertainty in locating the exact peak value of the output of the cross-correlator. If the autocorrelation function is sharply peaked, $R_s(\tau)$ will be much less than $R_s(0)$ for rather small values of τ, and the uncertainty in locating the peak will be less.

Therefore, as far as range measurements are concerned, the ranging signal is completely characterized by its autocorrelation function. Two particular examples are of special interest. The first is the autocorrelation

function given by $\cos \omega_m \tau$, the second is the one consisting of a periodic sequence of widely spaced narrow pulses.

Consider first the function $\cos \omega_m \tau$, which is the autocorrelation function of a tone of frequency ω_m rad/sec. The time shift between the peaks of $\cos \omega_m \tau$ is $2\pi/\omega_m$ sec, and each peak is contained within a fraction of this time separation. Therefore, the higher the value of ω_m the more sharply peaked $R(\tau)$ will be. Almost any degree of peakedness could be matched by the $R(\tau)$ of a single sine wave provided the necessary choice of ω_m is allowed.

But the higher the value of ω_m the smaller the time shift between peaks of $\cos \omega_m \tau$. Consequently, in almost all tracking situations of practical interest one cannot choose ω_m to be sufficiently high without violating the "ambiguity resolution" requirement that $2\pi/\omega_m$ exceed the round-trip transit time. A single sine wave of sufficiently high frequency to satisfy a desired degree of peakedness has an autocorrelation function made up of closely spaced, identical and indistinguishable sharp "pulses" each of which is perfectly suitable for phase coincidence. But no indication is provided as to which of the "pulses" is the desired one.

Alternately, one may consider an autocorrelation function made up of widely spaced narrow pulses with a zero or a uniformly low value in between. This type of autocorrelation function presents still another problem: it has the disadvantage of not providing any indication during the search process of which way and how far to shift the local replica of the delayed event in order to bring about the desired time coincidence.

When noise, bandwidth limitations and other practical considerations are taken into account, it will be found that the preceding two types of autocorrelation functions possess unique properties: the sine wave type is capable of meeting any preset precision requirement, whereas the widely spaced pulse type is capable of meeting any preset ambiguity resolution requirement.

The process of bringing the returned "event" and the local reference "event" in phase, or very close to it, is called acquisition. In the light of the above discussion, it is clear that a single precision-ranging sine wave is rapidly acquirable because of its relatively short period and the many positions in which it will be in phase with a time-shifted replica of itself. On the other hand, a waveform whose autocorrelation function is made up of isolated narrow pulses separated by long periods of uniformly low values may take much longer to acquire. The trial-and-error time in the acquisition process can be greatly reduced by not insisting upon "nothing" between the widely spaced pulses, but rather allowing the autocorrelation function to have intermediate pulses, or values, that are clearly distinguishable from the "in-phase" pulses or values and that clearly indicate the distance and direction to the nearest "in-phase" pulse.

In summary, the desired characteristics of the autocorrelation function, $R(\tau)$, of a signal for unambiguous precision range measurement may be set forth as follows:

a) $R(\tau)$ must be a narrow, sharply peaked pulse in the vicinity of $\tau = 0$ in order to minimize the uncertainty in locating the exact peak value of the output of the cross-correlator and hence reduce the corresponding range uncertainty.

b) The behavior of $R(\tau)$ in the interval between $\tau = 0$ and $\tau =$ (one period of the event) should be indicative of the direction in which τ should be changed in order to approach the $\tau = 0$ peak (and perhaps even of the magnitude of the desired change in τ), and

c) The period of $R(\tau)$ should exceed the two-way range signal propagation time.

2.2 Ranging Signal Synthesis Techniques

It is convenient to classify ranging systems into harmonic and non-harmonic. A harmonic system is based exclusively on characteristics

of sine waves such as their zero crossings or phase shifts. An important example of a harmonic ranging signal is one consisting of a number of low-frequency tones (sometimes called sidetones) whose frequencies are chosen so that the highest one meets the desired range-measurement accuracy, and the lower ones provide ambiguity resolution. Non-harmonic systems include all categories that are not centered exclusively on the properties of discrete sine waves in range measurement. Important examples are pulse radar and ranging systems based exclusively on pseudo-random binary sequences.

In harmonic systems, ambiguity resolution and high precision in the location of the peak of $R(\tau)$, together with "in between" indicators for rapid acquisition, can be accomplished by using a ranging signal consisting of several properly weighted tones. The autocorrelation function of such a sum of tones is a sum of cosine terms at the frequencies of the tones, all terms being cophasal at $\tau = 0$. Such an autocorrelation function possesses a tall peaked hump centered about $\tau = 0$. If the frequencies are harmonically related, this hump will repeat at intervals of the period of the lowest tone. The large humps are separated by a number of considerably smaller undulations that decrease in amplitude to a minimum near the mid-point between the humps. In the GRARR system, a number of tones are added whose frequencies are integer multiples in a geometrical progression of the lowest frequency. If the common multiple is M, the autocorrelation function of the sum is

$$R(\tau) = \sum_{n=1}^{N} a_n \cos M^{n-1} \omega_1 \tau \quad , \quad a_n \text{ real} \tag{1}$$

Let us now turn to some examples of non-harmonic signals. Consider first the single pulse. For a given resolution (limited maximum pulse-width) and a limitation on peak power, the available signal energy will be severely limited. Increased energy without sacrificing the accuracy of range determination may be secured by using a recurring group of short pulses and adding up the results of integrating over each pulse in a group. However, if the spacing between pulse groups is sufficient to prevent range ambiguity, the resultant peak factor will, in most practical cases, be so high that the available energy will still be severely limited.

The combination of the property of high signal energy that is characteristic of a continuous waveform with an autocorrelation function that is similar to that of a pulse train can be achieved by using a pseudo-random binary sequence. A recurring pseudo-random sequence of binary digits[3] can be generated by a clock-driven shift register. These sequences have roughly an equal proportion of ones and zeros, as would a random binary sequence, and they have a very sharp autocorrelation function. In fact, the autocorrelation function for a maximal-length shift-register sequence is characterized by the values

$$\begin{aligned} R(\tau) &= p \text{ for } \tau = kp, \; k = 0, \pm 1, \pm 2, \ldots \\ &= -1 \quad \tau \neq kp \end{aligned} \tag{2}$$

where p is the length of the sequence (= $2^n - 1$ for a shift register made up of n flip flops) and τ represents the shift (measured in binary digits). Thus a pseudo-random (sometimes denoted p-r) sequence with a long period, p, could be used to provide unambiguous and accurate range data. The unambiguous ranging capability of a coded sequence increases in direct proportion to its length; precision is determined by the width of each pulse in the sequence.

An important practical consideration affecting the use of p-r sequences is the time required to effect acquisition. The straightforward acquisition of a code by the receiver would involve a trial correlation with a shifted version of the transmitted waveform, with the average taken over a significant fraction of the total length of the code, for every possible shift until correlation is achieved. Because of the shape of the autocorrelation function, it is impossible to learn anything from a trial except that exact correlation has or has not been achieved. Then, assuming no prior knowledge of the target range, the mean acquisition time for a code p digits long would involve p/2 trial correlations. If the correlation properties of the code are to be fully realized, averaging must occur over the entire length of the code. But if the available signal energy relative to the background noise density is sufficiently high, reductions in the integration time may be allowed, resulting in a proportionate reduction of the acquisition time.

The above crude method may require as many as p trial correlations, while in principle, the fundamentals of maximal-length sequences show that the sequence carries only $\log_2 p \approx n$ bits of information and hence should, in the absence of noise, be completely determinable from one trial inspection of n digits. This, however, represents an extreme lower bound and is unrealistic because it assumes noise-free conditions.

When the signal energy relative to the background noise density is sufficiently high, the number of trials can be significantly reduced if the code is made up of several short subcodes that can be acquired individually. Several methods exist by which short sequences can be combined into a long sequence whose period is the product of the periods of the subsequences. If the lengths or periods of the subsequences are relatively prime, they can be combined linearly or nonlinearly (modulo 2 combinations of sequences of zeros and ones) to produce the required long sequence. For example, three sequences (subcodes) with relatively prime periods p_a, p_b, p_c can be combined to form a new sequence with period $p_w = p_a p_b p_c$, which can be acquired in at most $\sum_{i=a}^{c} p_i$ trials by direct correlation with each of the subsequences separately. This technique, however, has the drawback that while lining up each component subsequence, the full energy of the incoming signal is not employed, since the maximum height of the cross-correlation function between the combined sequence and one of its components is less than the height p of the autocorrelation function of the combined sequence. Thus, detectability is traded for speed of acquisition when such combined sequence techniques are used.

The acquisition time for each of the components depends on the number of elements over which the average is taken during each trial correlation. If the number of elements is small there may be considerable self-noise from the code appearing along with the random receiver noise. Correlation would have to be performed over the entire code period p_w to eliminate self-noise and to achieve the idealized correlation function of the code. As the length of the averaging interval is decreased, the acquisition time will decrease, but a point will be reached when the increased noise bandwidth and increased code self-noise begin to cause false acquisition indications.

2.3 Selection of Baseband Waveform and RF Modulation

The basic characteristics required of the "baseband" tracking "event" or signal have so far been discussed in terms of properties of the desired

autocorrelation function. However, it is well-known that an autocorrelation function is not sufficient for complete specification of a waveform. The complete design of the transmission system requires that we further specify

a) the choice of the baseband event waveform – specifically, the relationships among the frequencies, the initial relative phases, and the amplitude weightings of the baseband tones, or the elementary waveform in the p-r sequence; and

b) the modulation technique for placing the desired tracking signal in a specified region of the radio-frequency spectrum.

In the design of ranging signals, the choice of RF modulation affects the choice of baseband waveform. Consequently, we first seek to establish the desired type of RF modulation. We distinguish between linear modulation and exponent modulation.[4]

Linear Modulation

In general, linear modulation can be considered unsuitable for conveying a tracking signal. Although the signal occupies minimal bandwidth, it has several undesirable features. Any nonlinear amplification or signal processing in successive stages will give rise to crosstalk within the baseband. The power utilization inefficiency of linear modulations is a significant disadvantage. In the particular case of SSB modulated tracking signals, the use of product demodulation will introduce a baseband phase shift corresponding to any phase error existing between the nominal carrier and the reference.

An important exception is DSB with a suppressed or reduced carrier, generated by direct multiplication (or balanced-modulation) of the r-f carrier by a bipolar sequence of rectangular pulses. The result is equivalent to phase modulation by step functions. This type of modulation (well-suited for binary pseudo-random sequences) combines the advantages of linear modulation

and exponent modulation, as long as the binary waveforms are very nearly rectangular. (Excessive rounding of the edges of the binary pulses for economy of bandwidth occupancy brings out disadvantageous properties of linear modulation.)

Exponent Modulation

Although wasteful of frequency space when compared with linear modulation, exponent modulation offers the following advantages:

a) The peak factor of an exponent-modulated signal is the smallest achievable in an RF signal and is always considerably less than that of a linear-modulated signal. The constant signal envelope allows power amplifiers to be driven at their saturated levels in all transmitting or transponding units, resulting not only in the maximum output power levels, but also in increased amplification efficiency. Consequently, exponent modulation offers the maximum "power-packing" capability (or efficiency of packing of available average power into the radiated signal).

b) The system implementation is simplified because the signal can be processed in nonlinear devices and hence presents no problems of dynamic range of linear operation. (In practice, a dynamic range problem arises from the fact that the frequency characteristics of circuits depend upon signal level.)

c) In harmonic systems, the desired baseband sidetones can be extracted from the exponent-modulation signal in at least two ways:

   (i) by some exponent-demodulation means followed by appropriate phase-locked oscillator isolation of the desired tones; or

   (ii) by direct filtering operation on the IF signal spectrum and/or linear demodulation means.

In harmonic systems using exponent modulation, the use of exponent demodulation techniques prior to the isolation of the desired tones may result in important modifications of the noise spectral density as a function of frequency. Only under conditions of high input S/N ratio and with a phase demodulator does the baseband noise spectrum vary with frequency exactly in the same manner as the i-f noise spectrum varies with frequency deviation from the instantaneous signal frequency (e. g., white noise plus a carrier at the demodulator input leads to white noise at the demodulator output). But with a frequency demodulator under the same conditions, the output noise power spectral density is given by the i-f noise spectral density as a function of the frequency deviation from the signal instantaneous frequency, weighted by the square of this frequency deviation. Thus, white noise plus a much stronger carrier at the FM demodulator input leads to baseband noise having a parabolically rising power spectral density with increasing frequency.

When the S/N ratio is well below the demodulator threshold, the action of an FM demodulator (for example) upon the sum of signal plus noise leads to a substantial suppression of the signal and of the signal modulation. Thus, even though the desired tones may be present in the demodulator output deep in the noise, they can be expected to be less favorable to operate on than their first-order spectral contributions in the RF signal.

Consequently, direct extraction of the desired tones as frequency differences of specified IF spectral components possesses significant advantages. A 3-db improvement in performance against random noise as well as reduction of certain undesirable spectral components may be

achieved by using both the upper and the lower sideband components by translating the IF spectrum down to zero center frequency. One must, however, guard against a choice of modulating frequency (or frequencies) that results in an overcrowded spectrum for the resulting signal, thus complicating the problem of satisfactory isolation of the desired tones.

2.4 Comparison of Harmonic and Pseudo-Random Systems[2]

Careful consideration of the characteristics of tracking systems based on harmonic and pseudo-random signals brings out a number of points of great practical interest. First, in situations in which there is a decisive requirement for high resolution (or precision) and minimal acquisition time, with a limitation on allowable bandwidth occupancy, systems based purely on harmonic signals (or sidetones) are potentially superior to systems based exclusively on pseudo-random codes. Second, in situations in which there is a decisive requirement for resolving ambiguities in excess of a lunar distance, systems based purely on pseudo-random codes are potentially superior to those based exclusively on continuous tones. Third, from the viewpoint of all considerations influenced decisively by bandwidth occupancy, systems based exclusively on continuous tones are potentially preferable to those based exclusively on pseudo-random codes. Fourth, in situations in which there is a decisive requirement for transmission security and jam resistance, pseudo-random codes are clearly more advantageous. Fifth, in all respects other than those just enumerated, the two types of systems are of comparable ratings.

The advantages associated with each of the above two types of signals may be secured in a composite of harmonic and non-harmonic waveforms.

Representatives of this class of signals would range between

a) the extreme in which an all-harmonic signal is modified by the introduction of a low-frequency coded waveform for coarse ambiguity resolution, and

b) the extreme in which an all-pseudo-random code (or other non-harmonic) signal is modified by the addition of a single high-frequency sidetone for high resolution.

The optimal choice of hybrid signal would rely heavily on sidetones with an auxiliary ambiguity resolution function provided by p-r sequences or perhaps other pulse compression techniques. Such a composite system would allow the maximum range resolution (or precision) to be obtained from a signal of a given bandwidth without severely limiting ambiguity resolution. In addition, the signal acquisition time would be essentially that of a pure sidetone system.

A hybrid system would be particularly useful for tracking satellites in intermediate to lunar range orbits and in tracking all phases of a complex vehicle mission involving near-earth and deep space operations. It can also provide independent measurements of range and range rate at a rapid rate, which is particularly advantageous in tracking at lunar distances and beyond where relatively large round-trip transit times are encountered. The GRARR system was conceived to embody the advantages of a hybrid system in a manner that is readily adaptable to special mission requirements.

3. GRARR System Description

The Goddard Range and Range Rate System to be described in the present section combines the advantages of harmonic and pseudo-random signals in a highly effective and versatile manner, operable either as an all-harmonic system in near-earth orbital tracking or as a hybrid system for tracking more distant spacecraft.[5] The system also combines the utilization of the two types of signals in a very attractive technique for speeding up the process of acquiring the ambiguity resolving code component in tracking spacecraft at cislunar and translunar distances.

3.1 Overall System Description

A simplified block diagram of the GRARR System is shown in Fig. 1. The system utilizes both S-Band and VHF tracking equipment.

One mode of system operation is to use the S-Band portion of the system to extract range, range rate, and angle data and the VHF receiving system to guide the S-Band antenna in the initial spatial acquisition of the spacecraft. Thus, initially, the VHF antenna sector scans around the expected spacecraft approach angle until the VHF receiver locks onto the 136-137 Mc beacon transmissions from the spacecraft. During this operation, the S-Band antenna is slaved to the VHF antenna and the S-Band transmitter radiates an unmodulated carrier. When the VHF antenna acquires the spacecraft, the S-Band transponder is unsquelched by the S-Band uplink carrier and begins transmitting. The S-Band receiver then locks onto the satellite transmissions and automatically initiates the modulation of the uplink carrier with ranging tones, the S-Band antenna auto-track mode of operation, and the extraction of range, range rate, and angle data.

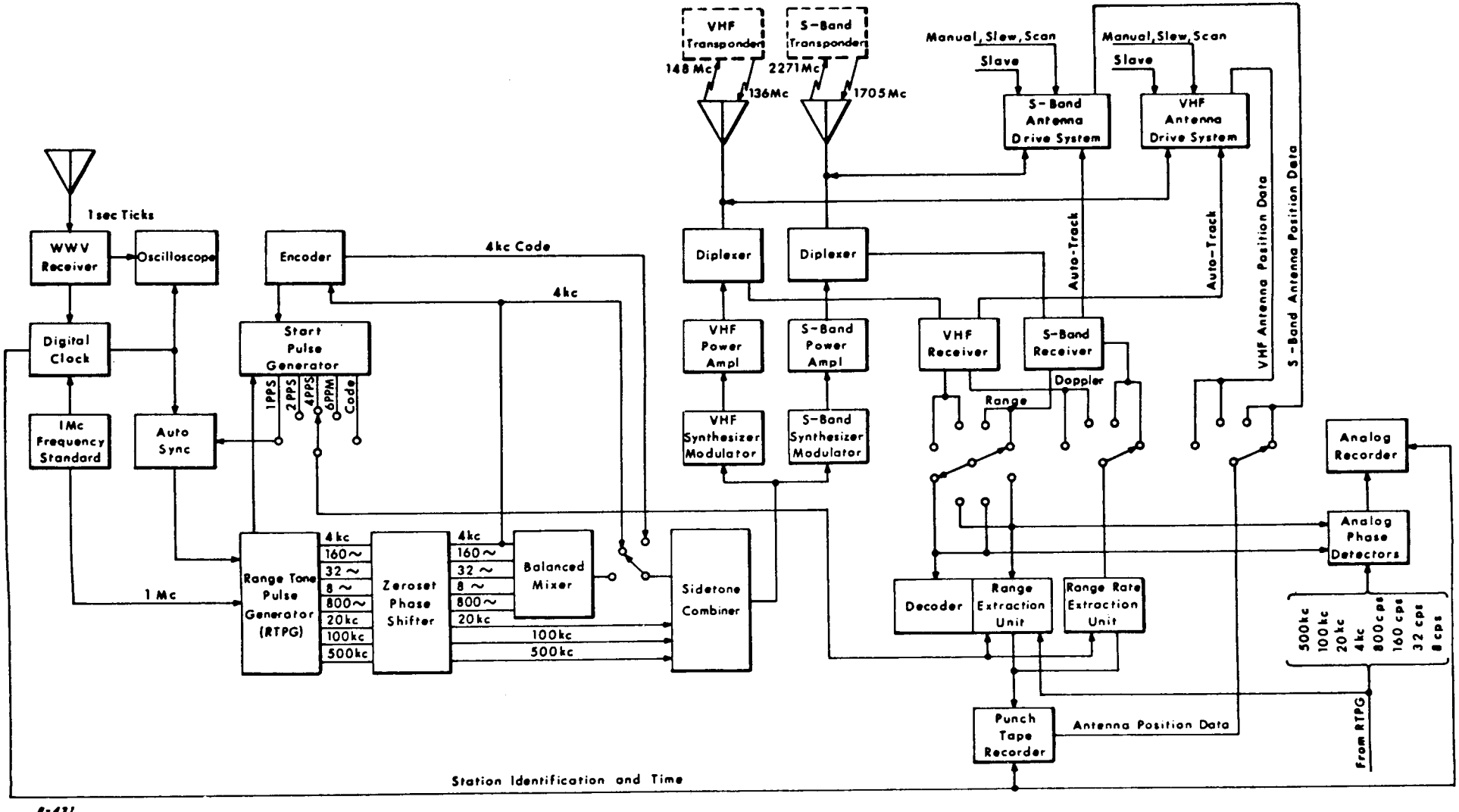

Fig, 1 GRARR system block diagram.

Another mode of system operation is to acquire and track at the VHF frequency. In this mode, the VHF antenna performs the sector scan until the VHF transponder carrier frequency is acquired by the VHF ground receiver. Then the antenna automatically reverts to an autotrack mode, range tones are applied to modulate the uplink VHF carrier and the VHF receiver starts extracting range, range rate, and angle data.

The sum of the ranging tones phase-modulates the uplink carrier. The transponder heterodynes the uplink signal in a double conversion process down to a pre-assigned sub-channel frequency space. Three separate bandpass amplifier-limiters are employed in the S-Band transponder in order to accommodate three-channel operation. The outputs from these amplifier limiters are summed and then applied as phase modulation on the downlink carrier. The downlink signal is thus PM/PM. Figure 2 shows the resultant spectra at the inputs and outputs of the S-Band and VHF transponders, respectively. The frequency translation and retransmission are performed in such a manner that coherent two-way doppler measurements can be obtained individually and separately by each ground station.

The VHF and S-Band ground antennas are mounted on identical hydraulically powered X-Y pedestals. The VHF antenna system consists of an array of cavity-backed slots mounted on a 28-foot square ground plane. It provides 20 db of gain at the 148 mc transmit frequency and 19 db at the 136 mc receive frequency. The outputs of the antenna elements are grouped and processed to generate one sum and two difference signals for phase-comparison monopulse angle tracking. The S-Band antenna system consists of two 14-foot parabolic reflectors with Cassegrain feeds so that the receive and transmit functions can be separated. It provides approximately 35 db of gain at the 2270 mc transmit frequency and 33 db at the 1705 mc receive frequency, and utilizes amplitude-comparison

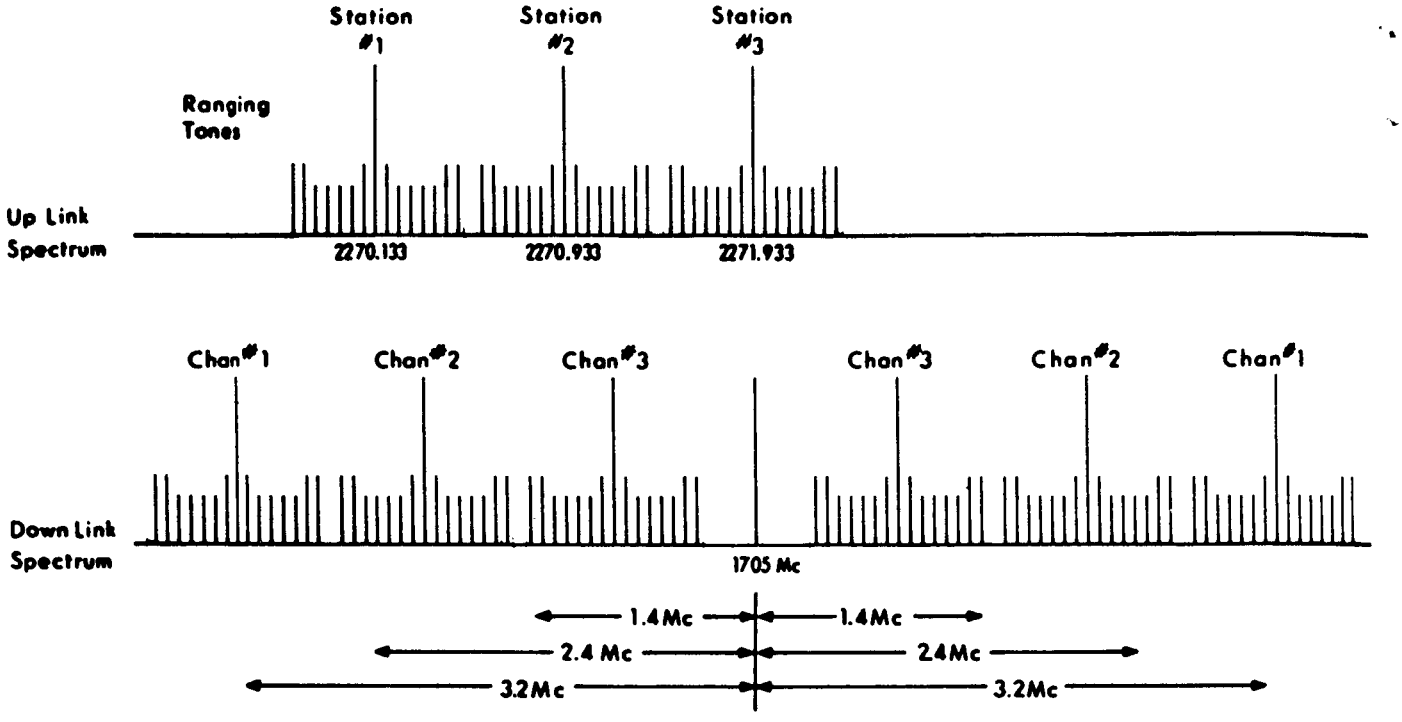

(a) Spectra of S-Band transponder input and output signals

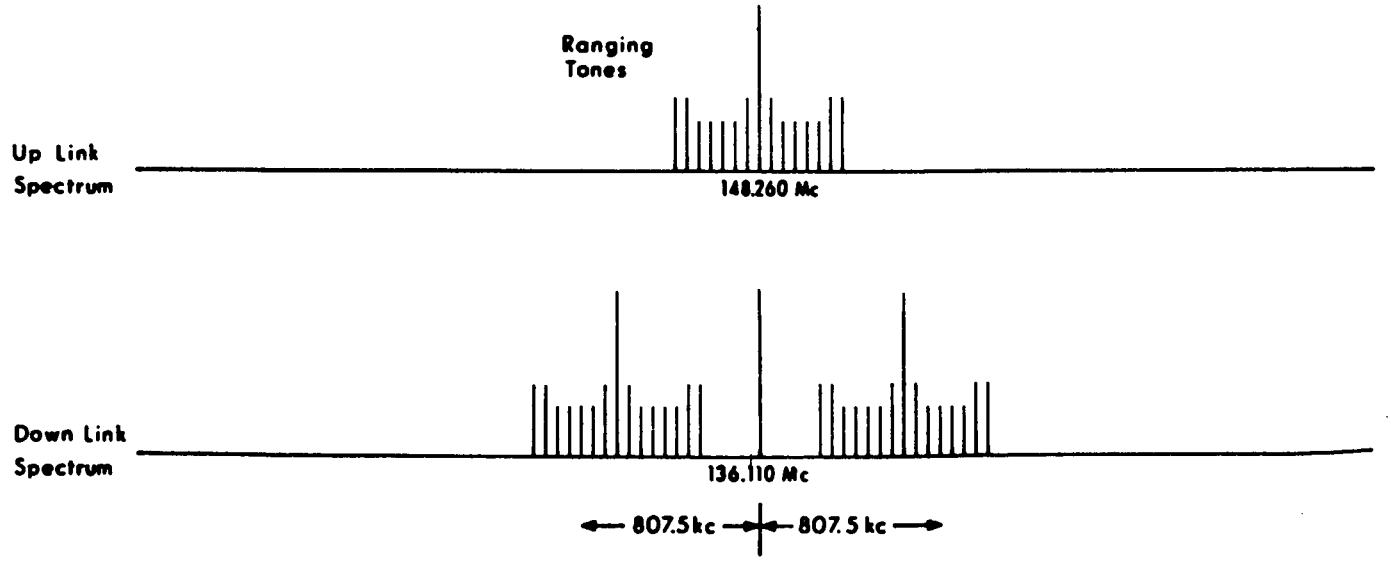

(b) Spectra of VHF transponder input and output signals

R-432

Fig. 2 Illustrations of GRARR signal spectra.

monopulse angle tracking. Two systems constructed after the initial program employ 30-foot parabolic reflectors with Cassegrain feeds for the S-Band antenna.

Associated with each antenna system is one sum-channel and two error-channel receivers. The sum-channel receiver contains the carrier and sub-carrier phase-locked loops. Its outputs consist of an AGC voltage and a reference signal for the error-channel receivers, a doppler plus bias signal for range rate extraction, and the demodulated range tones, ambiguity resolving code (ARC), and a rate-aiding signal for range extraction. The error-channel receivers provide synchronous amplitude detection of the X angle and Y angle tracking errors. The error signals drive a servo system that controls automatic angle tracking. A 16-bit angle encoder is used for precise angle read-out.

Range, range-rate and angle data are punched on paper tape, whence they are transmitted to GSFC via teletype in a format convenient for use in digital computing facilities for rapid, precise calculation of the space vehicle orbital parameters.

The VHF and S-Band systems radiate 10 kw each in their uplink signals. The power output is switchable to 500 watts in the S-Band system and 1 kw in the VHF system for close-in tracking, if necessary, to avoid transponder saturation.

A 1 Mc frequency standard provides extremely stable reference frequencies for the entire system. The digital clock provides a local time standard from the frequency standard and provides a 1 pps output for time synchronization with WWV. The system time accuracy is thus essentially limited by the uncertainty in propagation time of the WWV signal. The timing equipment is chosen to be several orders of magnitude better than this propagation uncertainty in order to allow for improved system timing

at a later date when a VLF WWV signal is made available with less propagation delay uncertainty.

The range, range rate, data multiplexing, and timing equipment are common to the two systems, allowing range and range rate measurements to be made with either the VHF portion or the S-Band portion, but not with both simultaneously.

3.2 Range Measurement (Sidetone)

Precision range measurements are accomplished by the use of ranging sidetones. The phase shift between ground-transmitted sidetones and transponder returned sidetones is directly proportional to the two-way range between the tracking antenna and the satellite. The ranging sidetone frequencies are 500 kc, 100 kc, 20 kc, 4 kc, 800 cps, 160 cps, 32 cps, and 8 cps. Thus, except for the last tone, successive frequencies are in a 5:1 ratio. (The considerations affecting the choice of tone frequency and frequency ratio among the tones are discussed in Section 4.) The highest frequency is selectable between 500 kc, 100 kc and 20 kc and is used to determine the finest increment of range; the lower-frequency tones are used to resolve range measurement ambiguities.

The reference pulse generator is used to produce phase-coherent tones of 100 kc, 20 kc, down to 8 cps. Reference pulses of 4 pps, 2 pps, 1 pps or 6 ppm are also generated. These tones and reference pulses are generated in a fully clocked digital divider chain using a 1 mc frequency standard signal as an input. Thus, each of the reference pulses is coincident with positive-going zero crossings of the higher tones. A reference pulse (selected with the system data rate switch), along with a zero crossing of the highest tone in use (100 kc in this example), is used to generate a start pulse that marks precisely the time of transmission of an all zero-phase condition for all the tones.

Prior to transmission, the ranging tones pass through the Zero-Set Phase Shifter Unit. This unit enables individual and combined phase shift of the ranging tones so that the individual transmitted tones can be phase- or time-shifted with respect to those used to generate the start pulse. In this way, an adjustable bias can be applied in the range time measurement to calibrate out the effect of fixed equipment time delays and differential time delays between tones.

The ground receiver uses an extracted carrier reference to shift the desired portion of the downlink RF spectrum down to a zero frequency center, filters the desired tones, and sends them to the Digital Tone Extractor. The Digital Tone Extractor regenerates clean tones that are phase coherent with the received tones in the following manner. The highest tone in use (100 kc in this example) is used to drive a digital divide chain that regenerates all the other tones (i.e., 20 kc, 4 kc down to 8 cps). The reconstructed 20 kc will be either in phase with the received 20 kc or some multiple of 360/5 = 72 deg out of phase with it (i.e., 72 deg, 144 deg, 216 deg, 288 deg). The phases of the digitally generated 20 kc and the received 20 kc are compared, and the digitally generated 20 kc is stepped in phase (by adding extra 100 kc pulses) until a zero phase difference is indicated. Once the 20 kc tone is locked, the 4 kc tones are synchronized in the same manner. This same process is used to phase synchronize all of the digitally reconstructed tones.

The use of this digital tone extraction technique makes it possible to switch off lower-frequency tones (in the sidetone combiner) after acquisition, since only the highest tone is required to drive the digital divide chain.

3.3 Range Measurement (Hybrid)

A maximal-length sequence is employed for resolving ambiguities when the transit time to the spacecraft and back is greater than the period

of the 8 cps sidetone. The resulting hybrid system[2,5] thus consists of the basic sidetone system modified to incorporate ambiguity resolution by a supplementary digital code ranging signal. Two independent range measurements are made, a tone range measurement and an ambiguity-resolving-code range measurement. The tone measurement uses tones from 500 kc to 8 cps, providing a precise range measurement that is ambiguous to an integral multiple of an 8 cps half wavelength (i. e., an integral multiple of 18, 740 km). The ambiguity-resolving-code signal is then used to resolve the 8 cps ambiguities in the tone range measurement out to approximately ~~606, 800~~ 1,215,600 km.

The ambiguity-resolving (henceforth abbreviated AR) code used in the GRARR system is a linear combination of two relatively prime maximal-length subcodes whose lengths are 127 bits and 255 bits. The combination produces an output sequence that repeats every 32, 385 bits and is driven at a clock rate of 4000 bits per second. This yields a code length of slightly over 8 seconds, corresponding to an unambiguous one-way range of ~~606, 800~~ 1,215,600 km.

A simplified functional block diagram of the hybrid system is shown in Fig. 3. The AR code is not applied until the tone system is completely acquired and tone ranging start and stop pulses are being generated. Once the tone system is acquired, the minor tones are removed from the transmitter and replaced with an AR-code-modulated 4 kc subcarrier. The first tone start pulse is used by the AR Decoder Control logic to simultaneously stop the AR Decoder and set its register contents equal to the contents of the transmitter AR Encoder. When the tone stop pulse is received by the control logic, the AR Decoder is started, using the doppler shifted 4 kc from the Digital Tone Extractor as a clock. Thus, the AR Decoder has been offset in time from the AR Encoder by the ambiguous two-way transit time to the spacecraft, as measured by the tone system. The AR

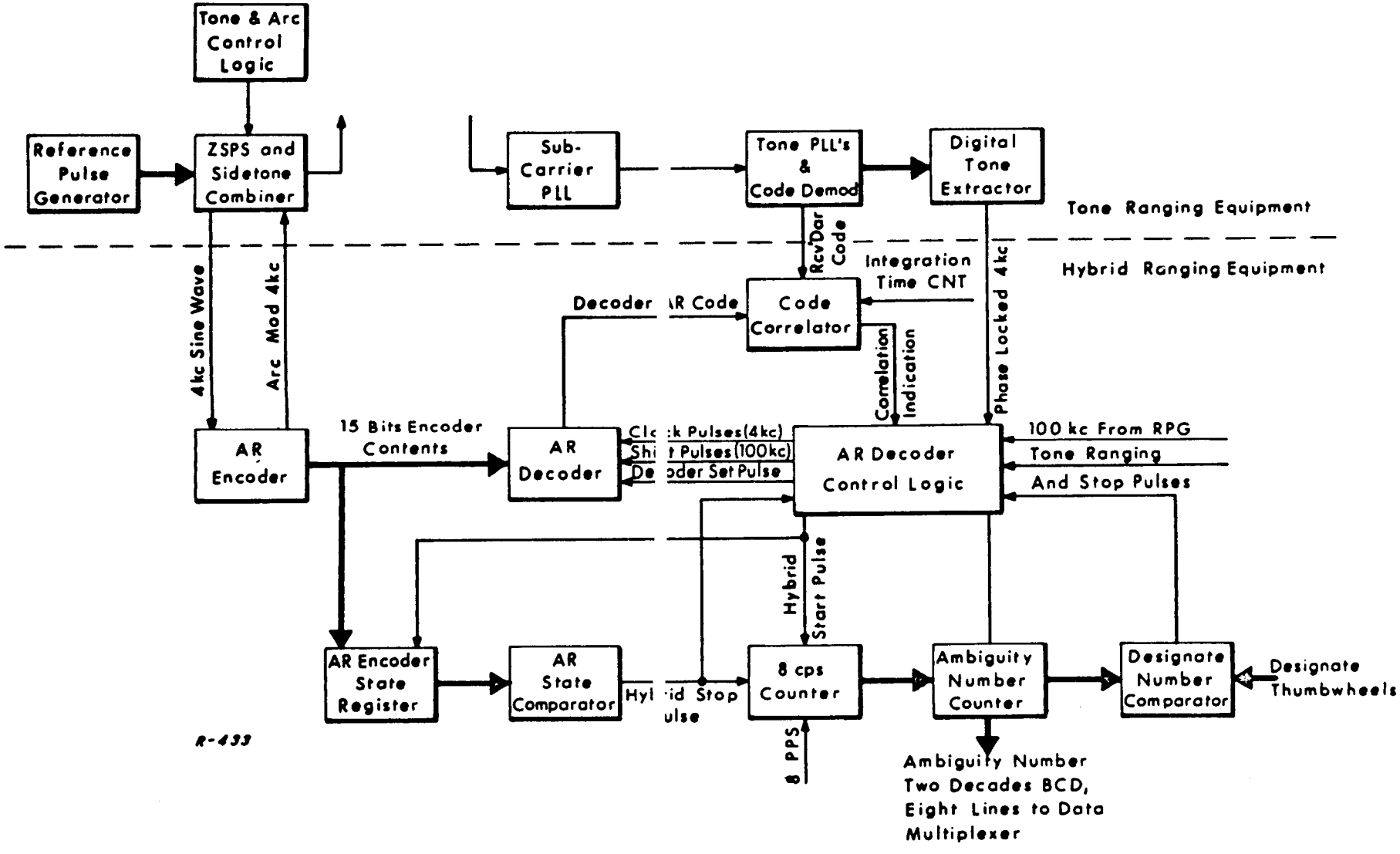

Fig. 3 Simplified functional block diagram of the hybrid ranging system.

Decoder will then be either in phase with the received demodulated code, or time-shifted from it by an integral number of 1/8 second (500-bit) intervals. The acquisition process now consists of making a trial correlation between the AR Decoder and the received AR code and if correlation is not indicated, stepping the AR Decoder by 500 bits (1/8 sec) and testing again for correlation. This process is repeated until correlation is achieved. The Ambiguity Number Counter receives a pulse from the decoder logic circuit each time the AR Decoder is stepped 500 bits, keeping track of the number of 8 cps periods involved. A set of thumbwheel digiswitches also enables the operator to start the acquisition sequence at any range ambiguity slot, allowing maximum use to be made of any a priori range information.

The method used to shift the AR Decoder in 500 bit steps is worthy of description here. It is desired to delay the AR Decoder 500 bits, which would require deleting pulses at a 4 kc rate if done in a conventional manner. Another way of achieving the same thing is to shift the code sequence forward through a whole sequence period minus 500 bits (i.e., 32,385-500 = 31,885 bits). Since the sequence used here is made up of two short subsequences, it can be shown[6] that by shifting the 255 bit subcode ahead 10 bits, and the 127 bit subcode ahead 8 bits, the composite code is shifted ahead 31,885 bits producing the desired 500 bit delay. Furthermore, since we are now adding pulses rather than deleting them, they can be added at a fast rate (100 kc) and the entire shift can take place between 4 kc clock pulses, thus minimizing the AR code shift time.

After correlation has been achieved and the hybrid system is completely phase-locked to the returned signal, the number in the Ambiguity Number Counter indicates the number of full 1/8 sec periods in the round-trip time to the spacecraft. The hybrid system now provides a continuous periodic check on this number so that it will automatically be updated when the spacecraft range changes to a new ambiguity slot.

3.4 Transponders

S-Band Transponder

The functional block diagram of the S-Band transponder is shown in Fig. 4a. The incoming signals are heterodyned down to pre-assigned subcarrier frequencies by mixing with a multiple of a locally generated reference signal. The reference oscillator frequency, f_o(=28.4167 mc), is used in a double conversion to translate a signal of up-link received carrier frequency f_{up} + $f_{up,d}$ to a subchannel at (80 f_o - f_{up} - $f_{up,d}$). Three subchannel frequency bands are used, centered at 1.4 mc, 2.4 mc, and 3.2 mc, corresponding to three different ground transmitter frequencies. This allows the transponder to be used by one, two, or three ground stations simultaneously. Each transponder subchannel contains bandpass amplifiers, limiters, and a squelch gate. The outputs of the subchannels in use are summed and used to phase-modulate the downlink carrier. The squelch gates keep unused subchannels from modulating the downlink carrier with pure noise. It should be noted that the transponder transmitter frequency is derived from the reference oscillator, f_o, which was used to generate the LO frequencies for the double conversion to subcarriers. This technique enables the downlink signal to be usable by the ground stations to extract two-way doppler for range rate measurement, free of the effects of the transponder reference oscillator instabilities, and without requiring separate telemetered information about spacecraft oscillators.

The design specifications of the S-Band transponder are given in Table I.

VHF Transponder

The VHF transponder is similar in operation to the S-Band unit, except that it is only capable of one-channel operation with 20 kc as the highest ranging tone frequency. This is primarily due to the lack of

bandwidth and frequency allocation in the VHF region. A functional block diagram of the VHF transponder is shown in Fig. 4b. The principal design specifications are presented in Table I.

The VHF transponder also serves as a telemetry transmitter for the spacecraft. The ranging function is energized by a command tone that allows the ranging modulation to be placed on the carrier. Thereafter, the presence of the 4 kc ranging tone holds the transponder in the ranging condition until the tones are turned off, at which time the transponder reverts back to a simple telemetry transmitter.

3.5 Range Rate Measurement

Range rate is determined from the two-way doppler shift of the uplink carrier frequency. In order to measure this doppler shift, it is necessary to maintain coherence of the up-link frequency through the transponder and back to the ground receiver where it is compared in frequency against a continuing sample of the uplink frequency in the range rate extraction unit. The range rate extraction unit measures doppler by counting a preset number of cycles of the sum of the doppler shift plus a known frequency offset, and determines the elapsed time through a time interval meter.

The uplink carrier is generated from an ultra stable 5.67 Mc crystal oscillator. By starting at approximately 5 Mc, as opposed to a higher frequency, better short-term stability can be achieved. This 5 Mc signal is frequency multiplied by 400 to produce an S-Band frequency, f_{up}. This signal is amplified, and radiated to the transponder, arriving as $f_{up} + f_{up,d}$ where $f_{up,d}$ is the one-way doppler on f_{up} resulting from the transponder range rate $\dot{r}$ and is given very approximately by

$$f_{up,d} = (\dot{r}/c) f_{up} \quad , \quad \text{for } |\dot{r}/c| \ll 1$$

The received signal is processed by the transponder, as described in Section 3.4, to generate a subcarrier ($80 f_o - f_{up} - f_{up,d}$) which is then used to phase-modulate a $60 f_o$ downlink carrier. This signal is transmitted down to the ground receiver where it is received with a doppler shift because of

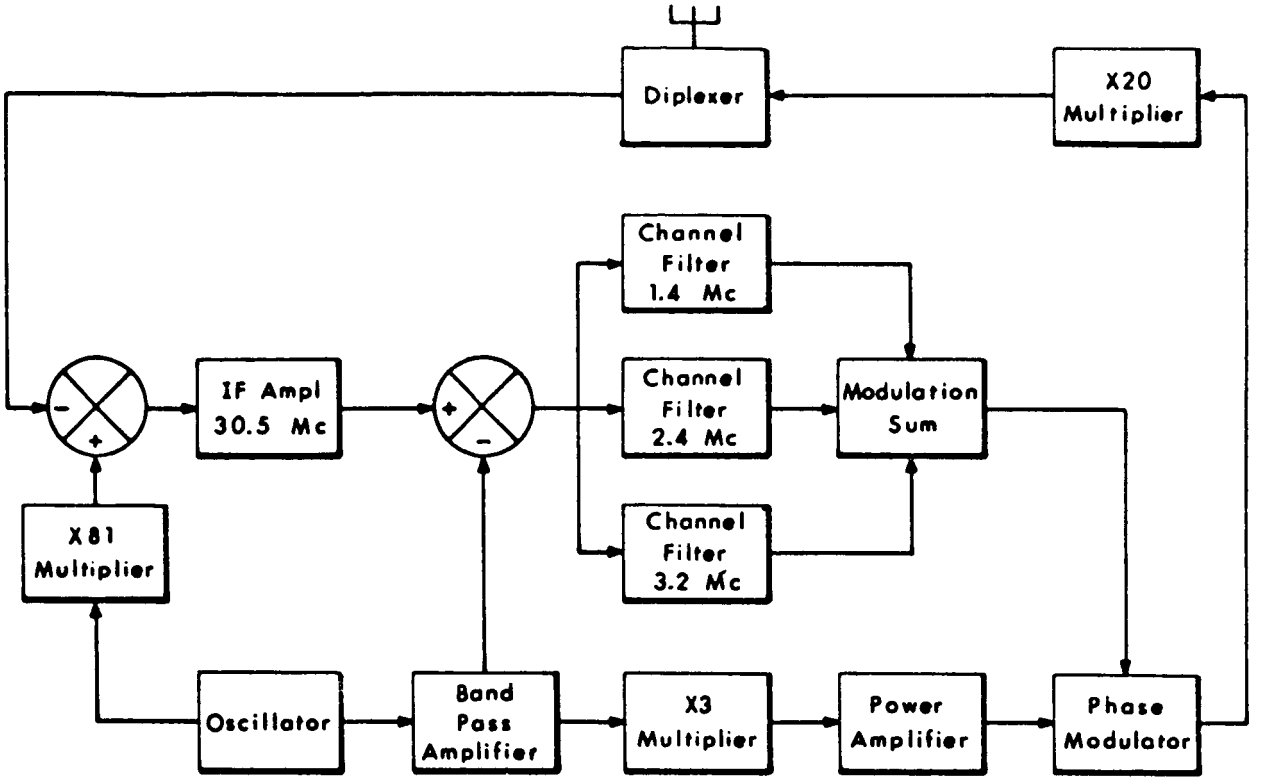

(a) S-Band transponder

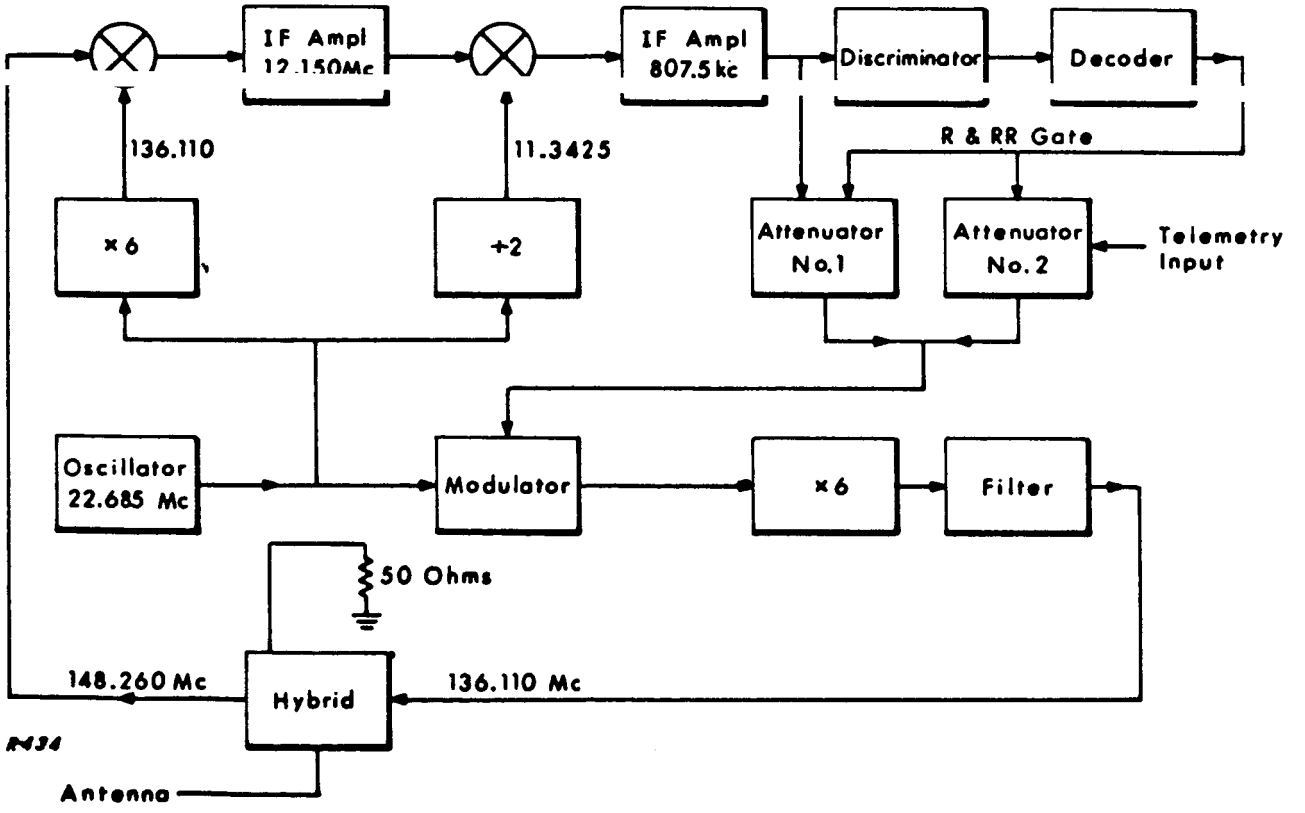

(b) VHF transponder

Fig. 4 Functional diagrams of GRARR transponders.

Table I

Design Specifications of GRARR Transponders

	S-Band	VHF
Input Signal Level	-40 dbm to -110 dbm (each channel)	-50 to -115 dbm
Input Frequencies	2270.1328 Mc 2270.9328 Mc 2271.9328 Mc	148.260 Mc
Channel Frequencies	3.2 Mc, 2.4 Mc, 1.4 Mc	807.5 kc
Channel Power Difference	0 to 32 db (any channel high)	----
Multiplication Ratio (transmit/receive)	3/4	12/13
Channel Information Bandwidth	400 kc	40 kc
Wideband Channel Bandwidth	3.3 Mc	----
Maximum One-way Doppler Shift	±85 kc	±5 kc
Transmitted Carrier Frequency	1705 kc	136.110 kc
Transmitter Power	1 watt	4 watts
Transponder Group Delay	4μsec (to within ±50 nanoseconds)	17 μsec
Noise Figure	12 db	8 db

transponder motion relative to the tracking station. The signal at the ground receiver has a carrier frequency of 60 $(f_o + f_{o,d})$ and a subcarrier frequency of $[80(f_o + f_{o,d}) - (f_{up} + 2f_{up,d})]$ corresponding to an original uplink frequency f_{up}. The objective of the ground receiver and doppler extractor circuit is to extract the $2f_{up,d}$ term, the coherent two-way doppler on f_{up}.

The receiver carrier loop locks a VCO to the incoming carrier providing a reference at $f_o + f_{o,d}$. The carrier loop "phase detector" also yields the subcarrier. The subcarrier loop phase locks a VCO to this subcarrier, producing a reference signal at $[80(f_o + f_{o,d}) - (f_{up} + 2f_{up,d})]$. The doppler extractor takes these two signals, along with the transmitter reference $f_{up}/80$ and combines them to produce $[500\text{ kc} + 2f_{up,d}]$. Thus, the desired $2f_{up,d}$ term has been obtained on a bias frequency of 500 kc. (The considerations that affect the choice of bias frequency are discussed in Section 4.) This doppler extraction process therefore tends to cancel out any instability or jitter on the transponder oscillator, f_o, provided that these instabilities are properly tracked by both carrier and subcarrier phase-locked loops.

The range rage extraction unit measures the time interval associated with N_o cycles of the bias plus doppler signal. When a reference pulse is received, a start pulse is generated to start the time interval unit counting 10 mc pulses. The start pulse also starts gating in cycles of bias plus doppler to the N_o-cycle counter. When N_o cycles have been counted, a stop pulse is generated to stop the time interval unit. The count 10-mc cycles in the time interval unit can be expressed as

$$N = \frac{N_o \times 10^7}{(f_b + 2f_{up,d})}$$

This count is made available to the Data Multiplexer in eight BCD decades (32 parallel lines). The two-way doppler can then be computed from a knowledge of N, the N_o used and the bias frequency f_b.

The VHF range rate measurement system is functionally the same as in the S-Band system. The major difference is that the VHF carrier and doppler frequencies are lower, resulting in lower values of N_o.

4 System Design and Performance Analysis

The purpose of this section is to provide a brief analysis of the design and performance of the GRARR system, with emphasis on the justifications for the selection of the critical design parameters and the special engineering considerations for precision tracking systems. The topics considered are:

(4.1) Characteristics of Trajectories
(4.2) Tracking Design and Performance Objectives
(4.3) Signal Analysis and Design
(4.4) Sources of Error
(4.5) Effect of Spacecraft Dynamics on System Design
(4.6) Fluctuation-noise Considerations

4.1 Characteristics of Trajectories

From the viewpoint of tracking system design, both the geometry of a trajectory relative to a tracking station as well as the dynamics of vehicle motion are of fundamental importance. The relative geometry and dynamics determine the maximum and minimum ranges and elevation angles, the maximum values of radial and angular velocity and acceleration, and the maximum "spectral extent" of the radial motion.

The GRARR system has been designed to track cooperative spacecraft in orbits ranging from near-earth to highly elliptical cislunar and translunar missions. The emphasis in the early system design was on highly elliptical orbits with high dynamics as typified by one with a 150 nautical mile perigee and a 60,000 nautical mile apogee. This orbit was picked for detailed analysis, inasmuch as it appeared to present the near extremes of GRARR mission dynamics. Analysis of the dynamics of this orbit yields a maximum range rate of about 10,000 meters/sec, which establishes a maximum two-way doppler of about 160 kc at 2271 Mc and

about 10 kc at 148 Mc. Maximum radial acceleration is about 400 meters/sec^2, establishing a maximum two-way doppler rate of about 6 kc/sec^2 at 2271 Mc, and about 400 cps/sec at 148 Mc. The maximum angular velocity is about 2 degrees/sec; the maximum angular acceleration is approximately 0.05 degree/sec^2.

4.2 Tracking Performance and Design Objectives

The performance of a tracking system is frequently specified in terms of:

(i) Resolution, which defines the tolerance on the exactness as limited essentially by random errors of all varieties.

(ii) Accuracy, which defines the tolerance on exactness as limited by instrumental imperfections and systematic errors attributable both to the equipment and to factors external to the equipment per se, such as the uncertainties in the knowledge of the velocity of light and of the positions of ground stations relative to one another.

(iii) Precision, which defines the number of significant figures to which a reading or a measurement can be made (e.g., a micrometer is a precision tool for measurement of length).

The specified performance objectives of the GRARR system call for the following rms tolerances on system instrumental accuracies:

	S-Band	VHF
Range	15 meters	50 meters
Range Rate	0.1 meter/sec	1.0 meter/sec
Angle	0.1 degree	1.0 degree

4.3 Signal Analysis and Design

We now turn to the signal analyses underlying the selection of range-tone frequencies and frequency ratio, AR code waveform and subcarrier modulation technique, doppler bias for range-rate measurement, and the RF signal modulation parameters.

4.3.1 Selection of Range-tone Frequencies and Frequency Ratio

The desired range-tone frequencies are determined by the requirements for (a) obtaining precision in the measurement of phase shifts; (b) resolving ambiguities; and (c) reducing the uncertainties of extraneous phase shifts.

A straightforward approach to the attainment of precision is through the use of digital time measurement techniques. If the phase shift of the demodulated sidetones is expressed as time delays, and the smallest resolvable increment is denoted ρ_t, the corresponding resolution of (one-way) range is $c\rho_t/2$ units of length, independent of the frequencies of the sidetones employed, where c is the velocity of propagation. In the GRARR system, time intervals are measured in quanta of 10 nanoseconds (which corresponds to 1.5 meters in range).

Resolving ambiguities usually requires that a sufficiently low periodicity be sought. Practical considerations of generation and processing discourage the use of range tones having frequencies much below 10 cps. The lowest frequency chosen for the GRARR system is 8 cps. This choice of lowest frequency provides for unambiguous ranging up to 18,470 km. If it were presently possible to measure the phase shift of 8 cps with sufficient accuracy, this single tone would suffice for all ranging requirements out to 18,470 km. In order to determine what phase-measurement accuracy

would be necessary with an 8 cps tone, let the system ranging instrumental accuracy be specified as $\pm\Delta R$ meters. Because of the uncertainty of $c\rho_t/2$ meters allotted to the time measurement, there would remain a maximum allowable uncertainty of $\pm(\Delta R - c\rho_t/2)$ meters ascribed to the measurement of 8 cps phase shift. This corresponds to a tolerance of $\pm(2\Delta R/c - \rho_t)$ sec in time delay measurement. The allowable phase error for a range tone of frequency f_R then becomes

$$\Delta\phi = \pm 360^{o} \times f_R \left(\frac{2\Delta R}{c} - \rho_t\right) \tag{3}$$

For $f_R = 8$ cps, $\Delta R = 15$ m and $\rho_t \ll 2\Delta R/c$

$$\Delta\phi \approx \pm 2.88 \times 10^{-4} \text{ degrees.}$$

It is not expected that the quality of tone isolation and drifts in the parameters of circuits that handle the 8 cps range tone could be maintained within these limits. But it is clear from Eq. (3) that the allowable phase error increases directly with the range tone frequency. For example, a 500-kc tone could have a maximum phase error of ±18 degrees.

The selection of the highest-frequency tone is governed by a number of requirements and constraints. These result from a specification of the desired instrumental accuracy, the "instrumental" S/N threshold above which this accuracy must be exceeded, and the limitation on allowable RF bandwidth occupancy.

Thus, let ΔR represent the maximum allowable instrumental uncertainty in the range measurement. Such a range error corresponds to a ranging-tone phase error of

$$\Delta\phi = 2\pi f_R(2\Delta R/c) \text{ rad} \tag{4}$$

where f_R is the ranging tone frequency in cps. Solving for f_R yields

$$f_R = \frac{c}{4\pi} \cdot \frac{\Delta\phi}{\Delta R} \tag{5}$$

Thus for a specified ΔR, f_R is determined by the maximum phase error $\Delta\phi$ that the system can be economically designed not to exceed.

Now, in any phase (or corresponding time) measuring scheme, the accuracy $\Delta\phi$ that can be achieved in making phase measurements is governed by the signal-to-noise ratio of the tone used. The tone must therefore be isolated by a narrowband filter from the wide band of noise corrupting a doppler-shifted spectrum. Phase-locked loops are desirable for this purpose because of their properties of narrowband filtering combined with frequency tracking. Under normal tracking conditions the closed-loop noise bandwidth may be made very narrow with respect to the frequency of the tone so that only the noise power contained in a small band of frequencies centered about the frequency of interest constitutes the disturbance of major importance. It can then be shown[7,8] that for $S/N \geq 7$ db, where S is the mean squared value of the isolated tone, and N is the mean squared value of the noise contained within the noise bandwidth of the phase-locked loop, the mean squared value of the phase noise on the isolated tone is closely approximated by

$$\overline{\phi_\epsilon^2(t)} = \frac{1}{2(S/N)} \tag{6}$$

The corresponding rms phase error in degrees is given by

$$\epsilon_{rms} \equiv \sqrt{\overline{\phi_\epsilon^2(t)}}/(2\pi/360) = \frac{40.5}{\sqrt{S/N}} \tag{7}$$

Thus, for a maximum tolerable rms phase error σ_ϕ we must ensure that S/N within the passband of the tone-isolation loop satisfies the condition

$$S/N \geq 1/2\sigma_\phi^2 \tag{8}$$

and for specified σ_ϕ and σ_R, the ranging-tone frequency f_R is given by

$$f_R = (c/4\pi)\,\sigma_\phi/\sigma_R \tag{9}$$

Substitution from Eq. (7) for σ_ϕ changes (9) to

$$f_R = \frac{0.056\,c}{\sigma_R\sqrt{S/N}} \approx \frac{c}{18\,\sigma_R\sqrt{S/N}} \tag{10}$$

Since approximation (6) holds only for $(S/N) \geq 5$ (≈ 7 db), this value of S/N is the lowest value that may be used in conjunction with Eq. (8) and (10). Plots of Eq. (10) for different values of σ_R are shown in Fig. 5. The curve for $\sigma_R = 15$ meters shows that this range accuracy can be maintained for $(S/N) \geq 21$ db if $f_R = 100$ kc, and for $(S/N) \geq 7$ db if $f_R = 500$ kc.

An upper limit on the permissible value of f_R is imposed by considerations of signal bandwidth occupancy, the coherence bandwidth of the transmission medium, and number of sidetones for a given frequency ratio between successive tones. In the design of the GRARR system, the coherence bandwidth of the medium has not been a serious consideration. The desire to limit the bandwidth occupancy to allow simultaneous multi-station operation with a relatively simple [illegible] of 100 kc as the precision tone frequency. For shorter range single-station operation, 500 kc has been chosen for the precision ranging tone

The choice of frequency ratio is governed by considerations of

a) S/N required for proper ambiguity resolution;

b) minimization of the effect of nonlinear processing of the sum of the tones upon the phases of the tones; and

c) number of tones acceptable from the viewpoint of signal power utilization, equipment implementation and operation, and occupation of allotted RF signal bandwidth.

From the viewpoint of S/N requirements, the phase of a given tone must be determinable with an accuracy that is sufficient for resolving one whole cycle of the tone of next higher frequency. The error specification must now be in terms of the peak tolerable error and the percent of

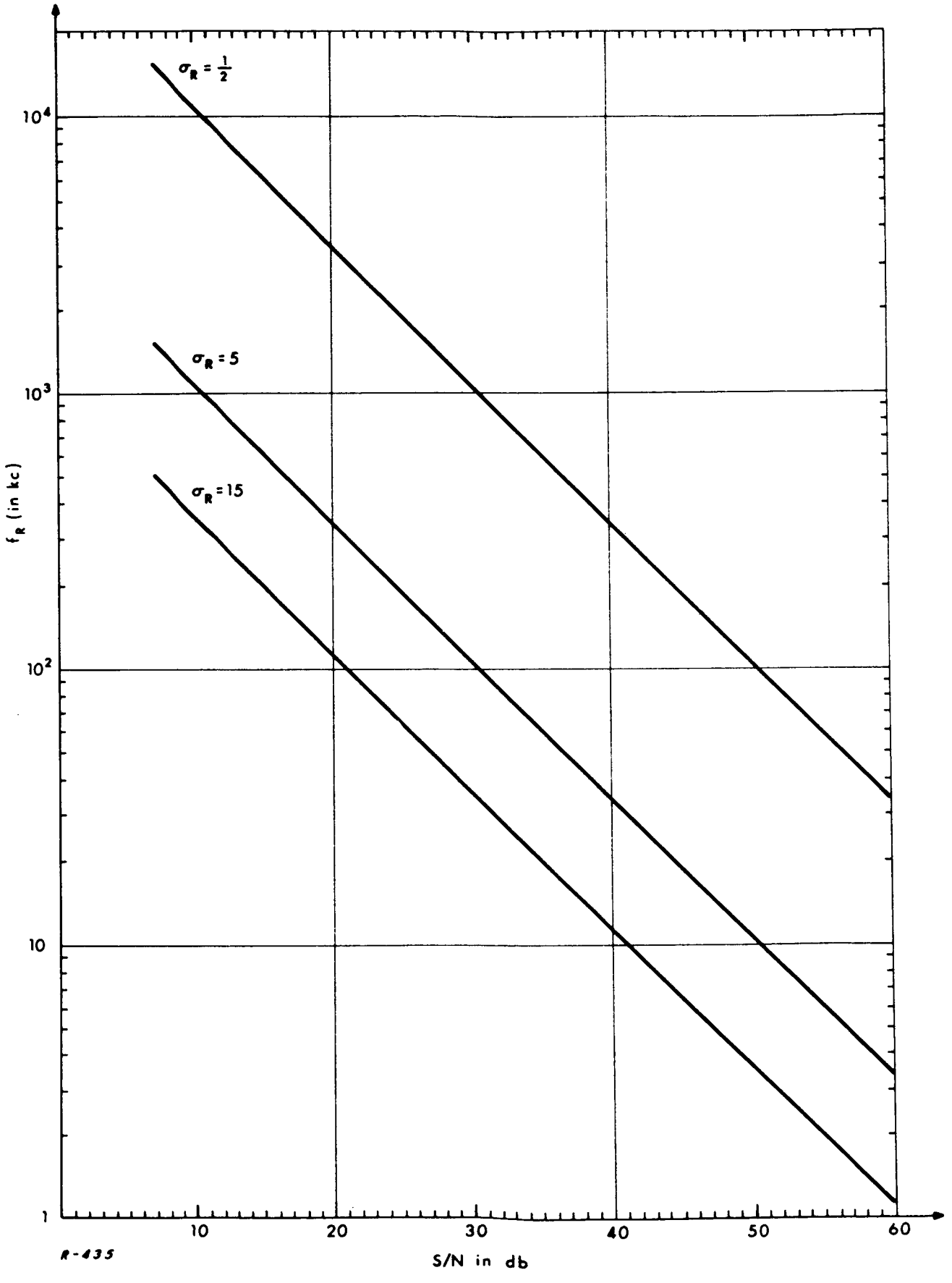

Fig. 5 Plots of ranging-tone frequency, f_R, required for meeting a specified rms range error tolerance σ_R.

time in which this tolerance is to be met. Thus, if the ratio of frequencies is 1:a(>1) then the maximum allowable instantaneous phase error is

$$\Delta\phi = \pi/a \tag{11}$$

The percent of time in which a specified level must not be exceeded by the noise is determined by the noise probability distribution and by the specified maximum level expressed in terms of a "peak factor" k (or in units of the rms value of the noise). A peak instantaneous error $\Delta\phi$ would then be equivalent to an rms error $\Delta\phi/k$. Thus we require that

$$\overline{\phi_\epsilon^2(t)} \leq (\Delta\phi/k)^2 \tag{12}$$

Combination of (6), (11) and (12) leads to

$$S/N \geq \frac{1}{2}\left(\frac{k}{\Delta\phi}\right)^2 = \frac{a^2k^2}{2\pi^2} \tag{13}$$

This condition shows that the lower the frequency ratio, a, the lower the threshold that must be exceeded by (and hence the less stringent the requirement on) the operating S/N.

It can also be shown that the higher the frequency ratio a the smaller the phase error that can result from nonlinear operations upon the sum of the tones.

But for specified highest and lowest tone frequencies, the smaller the frequency ratio the larger the required number of tones. A large number of tones is undesirable because of the equal number of required tone-isolation phase-locked loops and other auxiliary circuits and associated operational complexity. Moreover, the larger the number of tones, the less the available signal power per tone and the greater the occupancy of the available spectral space.

Within the above broad guidelines, a frequency ratio of 5 was considered a reasonable choice for the GRARR system.

4.3.2 ARC Modulation of 4 kc Subcarrier

For ambiguity resolutions requiring periodicities below 8 cps, all tones below 4 kc are disabled in the more recent GRARR systems, and a maximal-length ambiguity resolving code (ARC) is applied as a modulation on the 4 kc tone. The fundamental question regarding the generation of the ARC-modulated 4 kc signal is how to obtain, after phase modulation of the RF carrier, an RF spectrum that goes effectively to zero over a range of about ±300 cps centered at the carrier frequency. This property of the spectrum is desired as a necessary step for minimizing the disturbance to the carrier component of the phase-modulated RF carrier, the range of ±300 cps covering the selectable bandwidths of the carrier-isolating phase-locked loop. It must be noted at the outset that the nature of the phase-modulation process and the phase-modulating signal in the present application makes it impossible to free completely the immediate vicinity of the carrier component of interference, but the interference can be kept below tolerable limits if

a) the spectral density of the ARC-modulated 4 kc subcarrier is sufficiently low in the range of about ±300 cps about 0 cps; and

b) the phase deviation of the RF carrier by the ARC-modulated 4 kc tone is sufficiently small.

The type of ARC modulation of interest for the 4 kc tone is equivalent to a process whereby in each of a succession of time slots of duration 1/4000 sec one of two pulses p(t) or -p(t) is picked for transmission with equal probability. In such a situation, it can be shown that the mean-square spectral density of the resulting signal varies with frequency in direct proportion to the square of the magnitude of the Fourier transform of p(t).

The simplest and most effective modulation technique is to use the rectangular pulses of the ARC sequence to pick (with equal probability) a 4 kc sine pulse or its phase reverse to fill each of successive 1/4000-sec time slots. In this switching process, careful control of the switching time instants must be exercised in order to avoid transients resulting from amplitude and phase steps in the resulting ARC-modulated signal. Fortunately both of these undesired effects can be combated by switching only at zeros of the 4 kc subcarrier, and the amplitude steps and phase steps caused by unavoidable but small jitter can be kept below tolerable levels.

With careful control of the switching instants as just indicated, the spectrum of the resulting waveform is determined by the square of the magnitude of the Fourier transform of the sine-pulse. Direct computation of the resulting ratio of total power in the band extending ±300 cps around the carrier frequency to the power in the carrier component for the largest planned carrier phase deviation by the code yields approximately - 39 db.

4.3.3 RF Signal Design: Operating Frequencies, Modulation Parameters and Spectral Characteristics

The design of the RF signal is determined by the choice of uplink and downlink frequencies, the modulation parameters and the desired RF spectral characteristics.

The operating radio frequencies are determined on the basis of:

(a) The variation of environmental noise characteristics with frequency--e.g., sky noise, ground ambient noise, noise due to atmospheric and other absorption phenomena, etc.

(b) The availability of well-developed RF components, principally power amplfying devices that provide proper levels of power output.

(c) Compatibility with other operating earth and space systems.

(d) Considerations of range-rate measurement based on doppler shift of carrier frequency (which influence not only desirable frequency level but also the requirement of coherence between the up and down frequencies).

(e) Ground antenna gain characteristics as a function of geometrical dimensions versus frequency.

The combination of the above considerations has led to the selection of S-Band frequencies in the range of 1700 mc to 2200 mc, and VHF frequencies in the range of 135 mc to 155 mc. The up and down frequencies are in the ratio of 4 to 3 for S-Band and the ratio of 13 to 12 for VHF.

The modulation parameters are determined by

(a) the demodulation process, the one selected for the GRARR system involving direct use of particular RF spectral components in extracting the desired ranging waveforms (tones and ARC-modulated subcarrier);

(b) the requirement for a strong carrier component for rapid signal acquisition, for use in the monopulse system for angle measurement and antenna auto-tracking of spacecraft, and for use in range-rate measurements and as reference for extracting the desired ranging waveforms (tones and ARC-modulated subcarrier);

(c) the restriction on extent and density of bandwidth occupancy; and

(d) the desired distribution of signal power among the spectral lines corresponding to the various component ranging waveforms.

In what follows, analyses are provided of the RF spectral characteristics of signals that model the signals used in the GRARR system for bringing out their basic properties.

Basic RF Spectral Characteristics

Consider phase modulation by the composite signal.

$$e_m(t) = \sum_{j=1}^{M} A_j \sin[\omega_j t + \phi_j] \tag{14}$$

This represents the sum of M tones; the ARC-modulated 4 kc subcarrier may be included by an appropriate interpretation of the corresponding phase, ϕ_j. The resultant phase-modulated signal is given by

$$\begin{aligned} e_{PM}(t) &= \cos[\omega_c t + k_p e_m(t) + \phi_c] \\ &= \cos[\omega_c t + \sum_{j=1}^{M} k_j \sin(\omega_j t + \phi_j) + \phi_c] \end{aligned} \tag{15}$$

where $k_j = A_j k_p$. Since the k_j's are each less than unity, we can write

$$\begin{aligned} e_{PM}(t) \approx C_o \cos[\omega_c t + \phi_c] + \sum_{i=1}^{M} C_i \{ &\cos[(\omega_c + \omega_i) t + \phi_c + \phi_i] \\ &- \cos[(\omega_c - \omega_i) t + \phi_c - \phi_i] \} \\ &+ (\text{Smaller intermodulation terms}) \end{aligned} \tag{16}$$

where the amplitudes of the spectral terms are given by

$$C_o = \prod_{j=1}^{M} J_o(k_j) \tag{17}$$

$$C_i = J_1(k_i) \left[\prod_{\substack{j=1 \\ j \neq i}}^{M} J_o(k_j) \right] \tag{18}$$

In the GRARR system, the entire spectrum is translated by a linear product demodulation to a new center at zero frequency, where the desired tones are extracted by means of phase-locked loops. The spectrum of $e_{PM}(t)$ of Eq. (15) contains intermodulation terms of several types that may be large enough to be troublesome. Fortunately, the even-ordered intermodulation terms will cancel out in the necessary product demodulation operation if the inserted carrier is exactly in quadrature with the input carrier component. It must, however, be emphasized that imperfect cancellation of even-order terms may be expected because of improper phasing of the auxiliary carrier used in the detection process, due to inherent noisiness of the auxiliary detector carrier or a quasi-static phase offset caused by drifts and other phenomena. A phase deviation θ from orthogonality attenuates the odd-order terms by an amplitude factor of cos θ and the even-order terms by a factor of sin θ.

GRARR Uplink Signal

In the special case of the GRARR system there may be three uplink channels nominally separated in frequency by 1.0 mc and by 0.8 mc. Each channel may be operated in one of two modes, a parallel mode or a sequential mode. In the parallel mode, a channel is phase-modulated by a baseband signal containing seven sidetones. (The four lowest frequency ranging tones are complemented on the high side of the 4 kc tone, in order to ensure that no modulation frequency components lie so close to the carrier that they

would degrade carrier extraction and doppler measurement accuracy.) In the sequential mode, the baseband signal contains the highest-frequency tone all the time, the tones of lower frequency being switched on one by one in a sequence for a time sufficient to synchronize corresponding digital tone extractors, until finally the tone of lowest frequency or the ARC-modulated subcarrier is introduced. The 20 kc, 100 kc and 500 kc (when used) sidetones will hereafter be referred to as major sidetones and the remaining ones as minor sidetones (or minor frequencies to denote the 4 kc tone and the components spaced from it by the minor-tone frequencies). The carrier phase deviations selected for the various tones in each of the two modes of operation are listed in Table II. For S-Band sequential operation, the choice of deviations was based on maximizing the power in the highest-frequency tone subject to the constraints of equal carrier and subcarrier powers (for single channel operation) and minimum circuit complexity . For VHF, the deviations were chosen to maximize tone power without excessive degradation of subcarrier power and without increasing circuit complexity. In both cases, the carrier phase deviation by the code-modulated subcarrier is chosen so that replacing the minor tones with the code would not disturb the amplitudes of the other components present.

GRARR Downlink Signal

The GRARR S-Band transponder is designed to accommodate up to three simultaneously interrogating stations each of which uses a highest frequency not exceeding 100 kc for precision range measurement. The transponder may also accommodate only one station with a precision ranging tone frequency not exceeding 500 kc. Consequently, the downlink signal depends upon the number of active ground stations as well as upon the modulations carried on the associated uplink signals.

When more than one station are active at the same time, each uplink signal is first heterodyned down to a pre-assigned subcarrier frequency before it is applied along with the other heterodyned signals to the

Table II

CARRIER PHASE DEVIATIONS IN GRARR SIGNALS

Component	Parallel		Sequential	
	S-Band	VHF	S-Band	VHF
Up-link				
Major Tone (20, 100 and 500 kc)	0.7	0.7	-	-
Minor Tone (4, 4.008, 4.032, 4.160 and 4.800 kc)	0.2	0.7	-	-
Code-Modulated 4 kc	0.45	0.45	-	-
Highest Tone	-	-	1.06	0.7
Second Tone or Code	-	-	0.7	0.7
Down-link				
S-Band Subcarrier (1, 2 or 3 channel)	1.5, 0.75 or 0.5 (respectively)	-	1.5, 0.75 or 0.5 (respectively)	-
VHF Subcarrier	-	1.0	-	1.0

downlink phase modulator. Nominal subcarrier frequencies of 1.4 mc, 2.4 mc and 3.2 mc and a phase deviation of 0.5 rad of the downlink carrier for each of the subcarriers, have been chosen on the basis of occupying a bandwidth of less than 4 mc (for simplicity of transponder design) with a minimum likelihood of interference among the channels, and without seriously degrading the threshold S/N ratios for the desired spectral components. The magnitudes of the various terms in the downlink spectrum relative to the total power in the signal are listed in Table III. Numbers are also listed for sequential operation on the uplink signals and for VHF. These values refer to the components after spectral folding about $\omega = 0$. Note also that even-ordered intermodulation terms have been neglected since it is assumed that they are cancellable. Even-ordered terms actually exist in the spectrum with magnitudes up to -32.8 db.

4.3.4 Selection of Doppler Bias

In the GRARR system, range rate is determined from the doppler shift of the RF carrier frequency. The two-way doppler shift of a carrier used in tracking a space vehicle is expected to be small (of the order of a few parts in 10^5) compared to the signal frequency. Precise measurement of such a small fractional change in frequency may be facilitated by mixing the doppler-shifted incoming carrier component with a continuing replica of the originally transmitted signal and then operating on the resulting beat signal. Thus, if the incoming carrier component is, for simplicity, represented by $\cos[2\pi(f_c + 2f_d)t + \phi_c]$, and the local reference signal by $\cos[2\pi f_{ref}t + \phi_{ref}]$, the desired beat signal is given by

$$\cos\theta(t) = \cos[2\pi(f_c - f_{ref} + 2f_d)t + \phi_c - \phi_{ref}] \qquad (19)$$

Measurement of the frequency of this signal then yields the two-way doppler shift $2f_d$.

The measurement of the frequency of the signal represented by Eq. (19) may be performed by standard analog methods (such as a frequency

Table III

A. RELATIVE SIDEBAND POWER ON DOWNLINK S-BAND, PARALLEL MODE

Component	Total First-Order Sideband Power		
	1 Channel	2 Channel	3 Channel
Carrier	- 5.82	- 2.44	- 1.68
Subcarrier	- 5.80	-10.05	-13.13
Major Tone*	-11.36	-15.61	-18.98
Minor Tone*	-22.75	-27.00	-30.54
Code	-15.57	-19.82	-22.82

* In one-channel operation: 3 major and 5 minor tones.
* In two- and three-channel operation: 2 major and 5 minor tones.

B. RELATIVE SIDEBAND POWER ON DOWNLINK S-BAND, SEQUENTIAL MODE

Component	Total First-Order Sideband Power		
	1 Channel	2 Channel	3 Channel
Carrier	- 5.82	- 2.44	- 1.65
Subcarrier	- 5.81	-11.16	-14.16
Highest Tone	- 6.93	-12.28	-15.28
Second Tone or Code	-11.36	-16.71	-19.71

C. RELATIVE SIDEBAND POWER ON DOWNLINK VHF MODE

Component	Total First-Order Sideband Power	
	Parallel	Sequential
Carrier	- 2.33	- 2.33
Subcarrier	- 5.66	- 6.32
Major Tone (1)	-11.22	---
Minor Tone (5)	-22.61	---
Code	-15.32	---
Highest Tone	---	-11.88
Second Tone or Code	---	-11.88

discriminator) or by frequency counting methods. Analog measurement methods were discounted in the GRARR system design because they are less suited for high precision than frequency counting.

In considering any frequency measurement technique, it is important to note carefully the effect of the frequency $f_c - f_{ref}$ in Eq. (19) upon the measurement results. Thus, one may naturally consider choosing f_{ref} so that $f_c - f_{ref} = 0$ and perform the frequency measurement on

$$\cos[2\pi(2f_d)t + \phi_o - \phi_{ref}] \tag{20}$$

Such a choice however presents a number of difficulties. First, for small values of f_d in the presence of a given level of background noise, the measurement accuracy will be much less than for high values of f_d. Second, measurement of the frequency of a signal such as (20) does not yield the sign of the doppler shift, and hence no distinction is made between approaching and receding vehicles. Third, digital measurement approaches are based on either counting the number of cycles within a fixed time interval, T, or measuring the time interval T enclosed between specified zero crossings. The measurement breaks down in either approach as $f_d \to 0$. Finally, the proper implementation of high-speed doppler measurement instrumentation can be greatly simplified by choosing $f_c - f_{ref}$ so that the expected maximum negative value of the two-way doppler shift $2f_d$ does not bring down the instantaneous frequency of the sinusoid described by (19) too close to zero.

The above difficulties can be avoided by a proper choice of nonzero value for $f_c - f_{ref}$. The value of $f_c - f_{ref}$ in (19) will henceforth be denoted f_b and referred to as a frequency bias, or a doppler bias. If the doppler

frequency is "biased" by a frequency that is greater than the maximum expected negative doppler shift, the measured frequency would be higher or lower than the bias frequency, depending upon whether the vehicle were approaching or receding from the tracking station. The doppler frequency together with its sense may be determined later in the process of data reduction by subtracting the bias frequency from the measured frequency.

In the digital approach to the measurement, biased doppler is obtained from the ratio between number of cycles counted N and the time duration T for the count; namely,

$$\frac{N}{T} = f_b + 2f_d \tag{21}$$

where $2f_d$ is the two-way doppler frequency shift and f_b is the bias frequency. The technique may be implemented either for measuring "instantaneous frequency" (i. e., number of cycles per unit of a fixed counting interval) with a preset T and a changing N, or for measuring "instantaneous period" (i. e., time interval per cycle) with a preset N (defined by a specified sequence of zero crossings) and a changing T.

The counting approach based on a fixed small count of $f_b + 2f_d$ and the measurement of the resulting variable counting period T provides the preferred solution to the problem of precision measurement. Thus, a fixed small number, N_o, of cycles of cos $\theta(t)$ is chosen (independently of the instantaneous value of $\dot{\theta}(t) = f_b + 2f_d$) to define a time gate of variable width

$$T = \frac{N_o}{f_b + 2f_d} \tag{22}$$

The width T of the gate can be measured with high precision by using it to gate on a stable oscillation of much higher frequency than the biased doppler shift, and counting the number of cycles of this oscillation that are enclosed within the gate width. If f_{clock} cps denotes the frequency of the oscillation

used to "clock" the interval T, N is the resulting count of clock periods, and f_{clock} is chosen sufficiently high compared with the highest value of $f_b + 2f_d$, then

$$N = \frac{N_o f_{clock}}{f_b + 2f_d} \tag{23}$$

In Eq. (23), the number N_o and bias frequency f_b are design parameters that affect the quality of the doppler measurement, f_{clock} affecting only the ultimate precision of the time measurement. N_o is determined by the longest allowable counting interval T_{max}. This longest interval occurs when $f_b + 2f_d$ assumes its lowest expected value. Thus

$$N_o = T_{max}(f_b - 2f_{-d,\,max}) \tag{24}$$

where $-f_{-d,\,max}$ is the maximum expected negative doppler shift. T_{max} in turn is determined by spacecraft dynamics and required system accuracy (see Section 4.5). Substitution from Eq. (24) into Eq. (23) and solution for the error Δf_d resulting from an error ΔN in the count of f_{clock} cycles yields

$$\Delta f_d = \frac{-1}{2T_{max} f_{clock}} \cdot \frac{(f_b + 2f_d)^2}{(f_b - 2f_{-d,\,max})} \Delta N \tag{25}$$

Note that the factor multiplying ΔN determines the sensitivity of Δf_d to ΔN and that this factor is a maximum for $f_d = f_{+d,\,max}$ = maximum positive doppler shift. The choice of f_b that would make Δf_d least sensitive to ΔN at the higher end is

$$f_{b,\,opt} = 4f_{-d,\,max} + 2f_{+d,\,max} \tag{26}$$

Substitution in Eq. (25) yields

$$\Delta f_d = - \frac{(f_{d,p-p} + f_{-d,max} + f_d)^2}{T_{max} f_{clock} f_{d,p-p}} \Delta N \qquad (27)$$

where

$$f_{d,p-p} \triangleq f_{-d,max} + f_{+d,max}$$
$$= \text{peak-to-peak doppler shift} \qquad (28)$$

In the GRARR system, the various parameters used in the above analysis have been assigned the following design values:

$f_{-d,max} = f_{+d,max} = 0.83 \times 10^5$ cps

$f_b = 5 \times 10^5$ cps $\approx 6 f_{\pm d,max}$

$f_{clock} = 10^7$ cps

T_{max} = 97 msec for 8 samples/sec, S-Band system

= 6 msec for 8 samples/sec, VHF system

N_o = 32,751 for S-Band system, 8 samples/sec

= 2,046 for VHF system, 8 samples/sec

For sampling rates other than 8 samples/sec, the values of N_o are as follows:

Sampling Rate	S-Band N_o	VHF N_o
4 per second	65,503	4,093
2 per second	131,007	8,187
1 per second	229,263	14,328
6 per minute	3,133,956	182,182

4.4 Types and Sources of Error

A system error analysis serves a number of important objectives. First, it identifies the principal sources of error for careful consideration in design to minimize the contributions of individual sources and in system calibration prior to each mission. Second, on the basis of the cost (including difficulty, complexity, etc.) involved in reducing the contribution of each individual source, a logical basis is determined for subdividing a total allowable system error among the various sources, which often amounts to breaking down the overall system performance specifications to performance specifications for the various sub-systems. Third, it brings out the tracking accuracy that can be expected with a specified system design, and helps define the critical system check-out and evaluation tests.

System performance is limited by two general types of errors:

(i) Systematic errors. These are errors caused by unavoidable inadequacy of calibration, misalignments, drifts in circuit characteristics, uncertainty in knowledge of velocity of light, etc. Such errors are distinguished by consistency in value and direction during a typical tracking interval.

(ii) Random errors. These are errors caused by random-fluctuation disturbances, such as receiver noise, intercepted environmental noise, atmospheric fluctuations, etc.

Some of these errors are within the control of the system designer, some may be controlled by the system operator by proper calibration, some may be estimated or measured during system operation and hence compensated for in data processing, and some are caused by heretofore unresolved uncertainties.

The allowable error contributions of the various sources depend upon a variety of operational conditions as well as spacecraft dynamics. For illustration of typical comparative levels under ordinary conditions, a likely breakdown of instrumental errors in the GRARR system design is as follows:

Sources of Range Errors	Maximum Allowed Error
Thermal noise	7.5 m
Dynamic lags	0.3 m
Oscillator noise	0.2 m
Transponder group delay variation	7.5 m
Receiver delay variation	2.0 m
Oscillator calibration	0.5 m
Quantizing noise	0.6 m
Digital timing errors	5.0 m

Ambiguity resolution errors may be readily detected and corrected, unless the S/N ratio of the ambiguity resolving waveforms (tones or AR code) is too poor.

Sources of Range-Rate Errors	Maximum Allowed Error
Thermal noise	0.06 m/s
Coherent oscillator instability	0.022 m/s
Oscillator noise	0.01 m/s
Quantizing noise	0.036 m/s
Coherent oscillator calibration	neg.
Digital timing errors	0.029 m/s

4.5 Effect of Spacecraft Dynamics on System Design

In general, the motion of the spacecraft relative to a tracking station affects

a) the time it takes for spatial acquisition of the spacecraft by the ground antenna;

b) the time it takes the various loops in the system to acquire their respective signal components, and maintain proper lock (or tracking) of these components;

c) the total time the spacecraft is visible to the tracking station, and hence the bounds on allowable acquisition times;

d) the minimal sampling rate required, and the maximum allowable measurement time per sample, for extracting the data necessary for a satisfactory characterization of the trajectory and the motion;

e) the ultimate accuracy with which the data and the time of occurrence of a data sample can be determined; and

f) the possibility of interference between signals originating from two or more simultaneously interrogating stations, caused by the doppler shifts on the uplinks.

Of these considerations, only d) and e) are sufficiently critical in the GRARR system to deserve special discussion here.

Sampling Rate and Measurement Time

The minimum allowable sampling rate in the observation of a band-limited time function is determined by the width of the spectral region occupied by the function. In range and range-rate measurement, we are concerned with the spectral widths of r(t) and $\dot{r}(t)$, the time functions describing range and range rate. For the "typical" orbit considered in the GRARR system design it can be shown that the sampling frequency f_s must satisfy the condition

$$f_s > \frac{1}{\pi} \frac{|\ddot{r}(t)|_{max}}{|\dot{r}(t)|_{max}} \approx 1/80 \text{ samples/sec}$$

$$\approx 1 \text{ sample/minute} \qquad (29)$$

The lowest sampling rate used in the GRARR system is 6 per minute.

Another quantity that is limited by the spacecraft dynamics is the "measurement" time per data sample. In range measurement, the maximum allowable measurement time $T_{max,r}$ per sample is determined by the requirement that during this time the range should not change more than some fraction (say 1/10) of the specified system range accuracy, σ_R. Thus, if $\dot{r}_{max}$ = magnitude of maximum range rate, then we may require that

$$T_{max,r} \cdot \dot{r}_{max} \leq \sigma_R/10$$

whence

$$T_{max,r} \leq \sigma_R/10\dot{r}_{max} \tag{30}$$

Similarly, for range rate

$$T_{max,\dot{r}} \leq \sigma_{\dot{R}}/10\ddot{r}_{max} \tag{31}$$

The design numbers mentioned in Sections 4.1 and 4.2 yield

$$T_{max,r} \leq 0.15 \text{ msec, and } T_{max,\dot{r}} \leq 0.025 \text{ msec} \tag{32}$$

In range measurement, $T_{max,r}$ is the maximum allowable sum of delay in the transponder, delay in the ground receiver between antenna and tone PLL's, and integration time of the PLL of the highest-frequency tone in the ground receiver. In the GRARR system, the delays in the transponder and in the ground receiver prior to the tone PLL's are determined by bandwidths that are very much wider than the tone PLL bandwidth, and hence may be neglected relative to the closed-loop integration time. The PLL closed-loop integration time is optimized for a suitable compromise between random-noise error and dynamic lag error.

In range-rate measurement, we require that the time delay $\tau_{d,transp}$ in the transponder plus the time delay $\tau_{d,g}$ in the ground receiver prior to biased-doppler counting, plus the maximum value T_{max} of Eq. (24) of the doppler counting interval, satisfy the condition

$$\tau_{d,transp} + \tau_{d,g} + N_o/(f_b - 2f_{-d,max}) \leq \sigma_{\dot{R}}/10\ddot{r}_{max} \tag{33}$$

In the GRARR system, $\tau_{d,\,transp}$ is about 4 μsec in the S-Band system and about 17 μsec in the VHF system, $\tau_{d,\,g}$ is principally determined by a 100-cps wide crystal filter for the ranging tone, and by a carrier-tracking loop with a bandwidth having one of the lower values from the set {2000, 600, 200, 60, 20 cps} for the biased- doppler tone.

It is to be noted, however, that the system accuracy is normally expected to deteriorate under the peak dynamic conditions (high values of range rate and radial acceleration), because the system calibration is made under quasi-static conditions, leaving all response errors under the peak dynamic conditions uncompensated for. This suggests that a more relaxed bound on the measurement time than is indicated above may be justified under the more severe dynamic conditions. The errors caused by mildly excessive measurement time may also be partially compensated for in data processing.

Ultimate Sample Timing and Data Accuracy

The steps performed in the measurement of each sample value of range are as follows: First, a time interval start pulse is generated by the coincidence of a reference pulse (selected with the data rate switch) and a positive-going zero crossing of the highest ranging tone in use. With proper pre-alignment of the tones, the start pulse marks the instant of transmission of the "event" "all tones are in phase". After return via the transponder, the received tones are applied to the Digital Tone Extractor for regeneration of clean tones phase coherent with the returned tones. The positive-going zero crossings of the regenerated tones are then used to generate a stop pulse that marks the instant of reappearance of the "event""all tones are in phase" back at the receiver. The time separation between the start and stop pulses is taken as the round-trip transit time to the transponder. This time separation is measured in the Time Interval Unit by counting the number of 100 mc periods enclosed within it.

The round-trip transit time is therefore measured in quanta of $1/10^8$ sec = 10 nanoseconds. The counting time interval for each sample is equal to the round-trip time to be measured.

Two questions may therefore be raised. The first concerns the effect of the time it takes the ranging "event" to travel to the spacecraft and back to the point of measurement upon the definition of the time of occurrence of a data sample; the second concerns the ultimate data accuracy.

The same questions also arise in connection with range-rate data, where an interval of time is measured as defined by a preset number of cycles of the biased-doppler tone, as discussed in Section 4.3.4.

The first question concerns the "age" of a datum point by the time it has been measured. Corrections must evidently first be made for the inevitable but closely predictable delays in the transponder and the ground equipment. After such delays have been properly accounted for, one may reasonably assume that each range reading should be assigned to the instant of time at the mid-point of the round-trip transit interval, and each range rate reading should be assigned to the instant of time occurring a one-way transit interval before the start of the counting interval. In each case, it should be clear that the assigned instants of occurrence of the samples will not be uniformly spaced and the "age" of the information will change from sample to sample, because of the changing value of the one-way transit time. Moreover, the up transit time and doppler will be different from their down values if the delay in the transponder is not properly bounded in terms of range rate and acceleration, causing the above assignment of data points to instants of occurrence to be in error.

The data accuracy is limited in the measurement techniques by the automatic quantization as well as the fact that range and range rate will change during the delays and the counting times.

In the range measurement, the round-trip time is measured in quantum steps of 10 nanoseconds, resulting in an rms quantization error of of $10/\sqrt{12}$ nanoseconds (equivalent to 0.42 m).

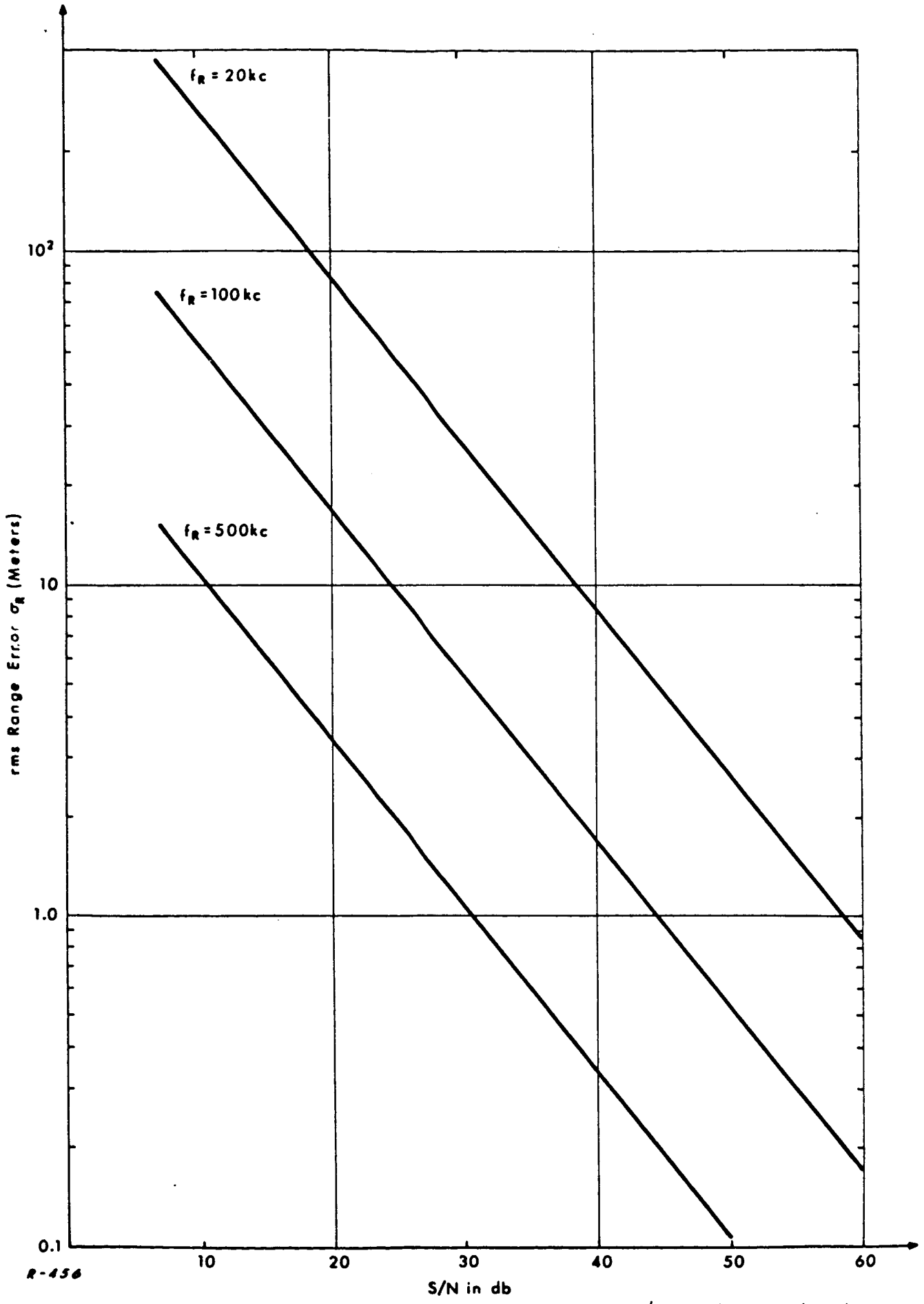

Fig. 6 Plots of rms range error σ_R as a function of S/N in the ranging-tone isolation filter bandwidth, for different ranging-tone frequencies, f_R.

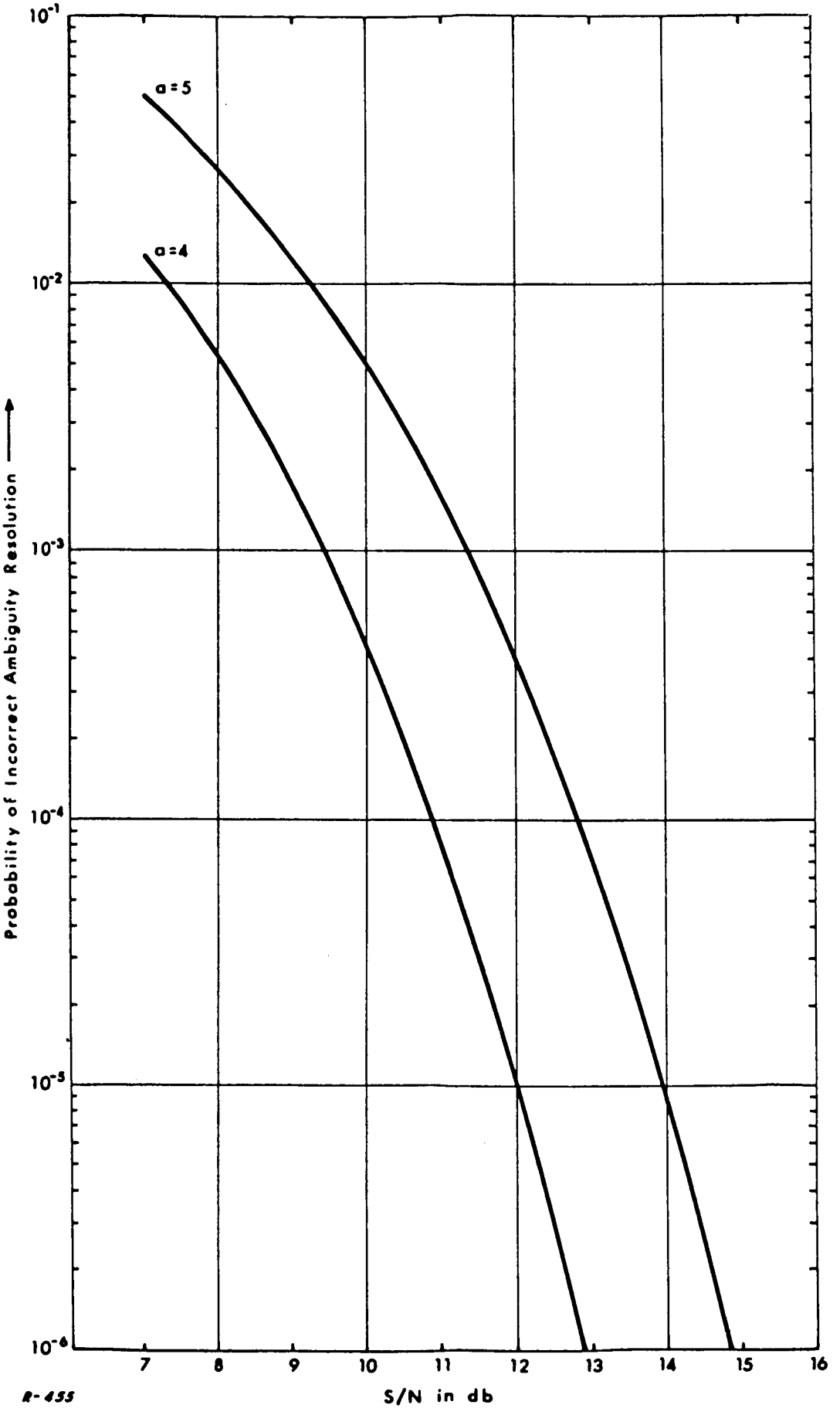

Fig. 7 Plots of probability of incorrect ambiguity resolution as a function of (S/N) in the tone-isolation filter bandwidth.

The cycle counting technique for measuring doppler also results in quantized data. In order to derive an estimate of the resulting quantization error we first observe that the count N changes by one for each "quantum" change in the instantaneous doppler shift. Consequently, the quantum step in the range-rate measurement is, from Eq. (25), given by

$$(\Delta \dot{r})_{\text{quantum}} = \frac{c(f_b + f_d)^2}{2T_{\max}(f_b - f_{-d,\max}) f_{\text{ref}} f_{\text{up}}}$$

where f_{up} = the uplink carrier frequency radiated by the ground transmitter. The size of the step is seen to depend upon f_d and to be maximum for the maximum value of f_d. Thus, if we set $f_d = f_{+d,\max}$ and $f_b = f_{b,\text{opt}}$ of Eq. (26), we obtain

$$(\Delta \dot{r})_{\text{quantum, max, opt}} = \frac{4cf_{d,p-p}}{T_{\max} f_{\text{up}} f_{\text{clock}}} \tag{34}$$

Therefore, the rms range-rate quantization error is less than or equal to

$$\frac{2cf_{d,p-p}/\sqrt{3}}{T_{\max} f_{\text{up}} f_{\text{clock}}} \tag{35}$$

For the design numbers listed in Section 4.3.4 for the S-Band system (f_{up} = 2270 Mc), the bound given by (35) is approximately 0.025 m/sec.

4.6 Fluctuation-Noise Considerations

The effect of random-fluctuation noise passed by a tone-isolation filter upon the observed phase of the tone was discussed in Section 4.3.1. In the present section we shall use the results of Section 4.3.1 to determine the S/N requirements for the precision ranging tones, the ambiguity resolving tones and the biased-doppler measurements. Plots will be presented that provide guidance in the distribution of signal power among the ranging tones, and the selection of carrier isolation bandwidths for the doppler measurements.

4.6.1 S/N Requirements for Precision Range Tones

From Eq. (10), the rms range error σ_R as a function of the ranging-tone frequency f_R and tone S/N ratio within the tone-isolation PLL bandwidth is given by

$$\sigma_R = \frac{0.056c}{f_R\sqrt{(S/N)}} \quad , \quad (S/N) \geq 7\text{db} \tag{36}$$

where c is the velocity of signal propagation. This expression is plotted in Fig. 6 for the three major tones. Inspection of this plot shows that for a specified σ_R of 15 meters, S/N must exceed 7 db for f_R = 500 kc, 21 db for f_R = 100 kc and 35 db for f_R = 20 kc.

Actually, the threshold value for rms error due to additive random-fluctuation noise should be taken as less than the specified 15 meter system accuracy because of the many other sources of non-negligible error. A representative division of total error budget among the various error sources was presented in Section 4.4.

4.6.2 S/N Requirements for Ambiguity Resolving Tones

If gaussian noise and (S/N) $\geq$ 7 db are assumed, then the probability that the phase error $\phi_\epsilon(t)$ on an ambiguity resolving tone will exceed k times the rms value ϵ_{rms} of the error is given by

$$P(\phi_\epsilon > k\,\epsilon_{rms}) = 1 - \text{erf}(k/\sqrt{2}) \tag{37}$$

Now, if the frequency ratio between successive tones is a, then for proper ambiguity resolution, the phase error on an AR tone should, from Eq. (17), be less than π/a rad. Therefore, the probability that an AR tone will not correctly resolve the ambiguity on the next higher-frequency tone is given by

$$P(\phi_\epsilon > \pi/a) = 1 - \text{erf}\left[(\pi/a)\sqrt{S/N}\right] \tag{38}$$

where we have combined Eqs. (9), (17) and (37). Equation (38) is plotted for a = 5 and a = 4 in Fig. 7.

Inspection of Fig. 7 shows that for a probability of incorrect ambiguity resolution of 10^{-5} or less, the S/N ratio must equal or exceed 12 db if a = 4 and 14 db if a = 5.

From Figs. 6 and 7 it is clear that the precision tone must be favored with considerably more signal power than the ambiguity resolving tones.

4.6.3 S/N Requirements for Biased Doppler Tone

The biased-doppler tone derived from the returned carrier component will be accompanied by a narrowband of random-fluctuation noise. If a slowly changing doppler is assumed, the instantaneous frequency of the biased-doppler tone can be expressed as

$$f_b + 2f_d + f_n(t) \equiv f_{bd} + f_n(t) \tag{39}$$

where $f_n(t)$ is the fluctuation introduced by the noise. Consequently, the expression for the count of $1/f_{clock}$ periods becomes

$$N = \frac{N_o f_{clock}}{f_{bd}[1 + f_n(t)/f_{bd}]} \approx \frac{N_o f_{clock}}{f_{bd}} [1 - f_n(t)/f_{bd}] \tag{40}$$

since $|f_n(t)| \ll f_{bd}$. If a constant input mean-square noise density is assumed and the spectrum of $f_n(t)$ is limited to within $\pm B_n/2$ cps of zero frequency, it can be shown that for a range-rate error of $\sigma_{\dot{R}}$ or less, S/N must satisfy the condition

$$\sqrt{(S/N)} \geq \left(\frac{cN_o B_n}{8\sqrt{6}\, T_{max} f_{up} f_{d,p-p}} \right) \Big/ \sigma_{\dot{R}} \tag{41}$$

which holds for S/N $\geq$ 10 db. Figure 8 presents a plot of $\sigma_{\dot{R}}$ as a function of S/N according to the equality sign in (41) and for the choice of GRARR design parameters given in Section 4.4.4. and f_{up} = 2270Mc. This plot shows that for $\sigma_{\dot{R}}$ of 0.1 m/sec, (S/N) must equal or exceed about 9db, if B_n = 20 cps and 32db, if B_n = 300 cps.

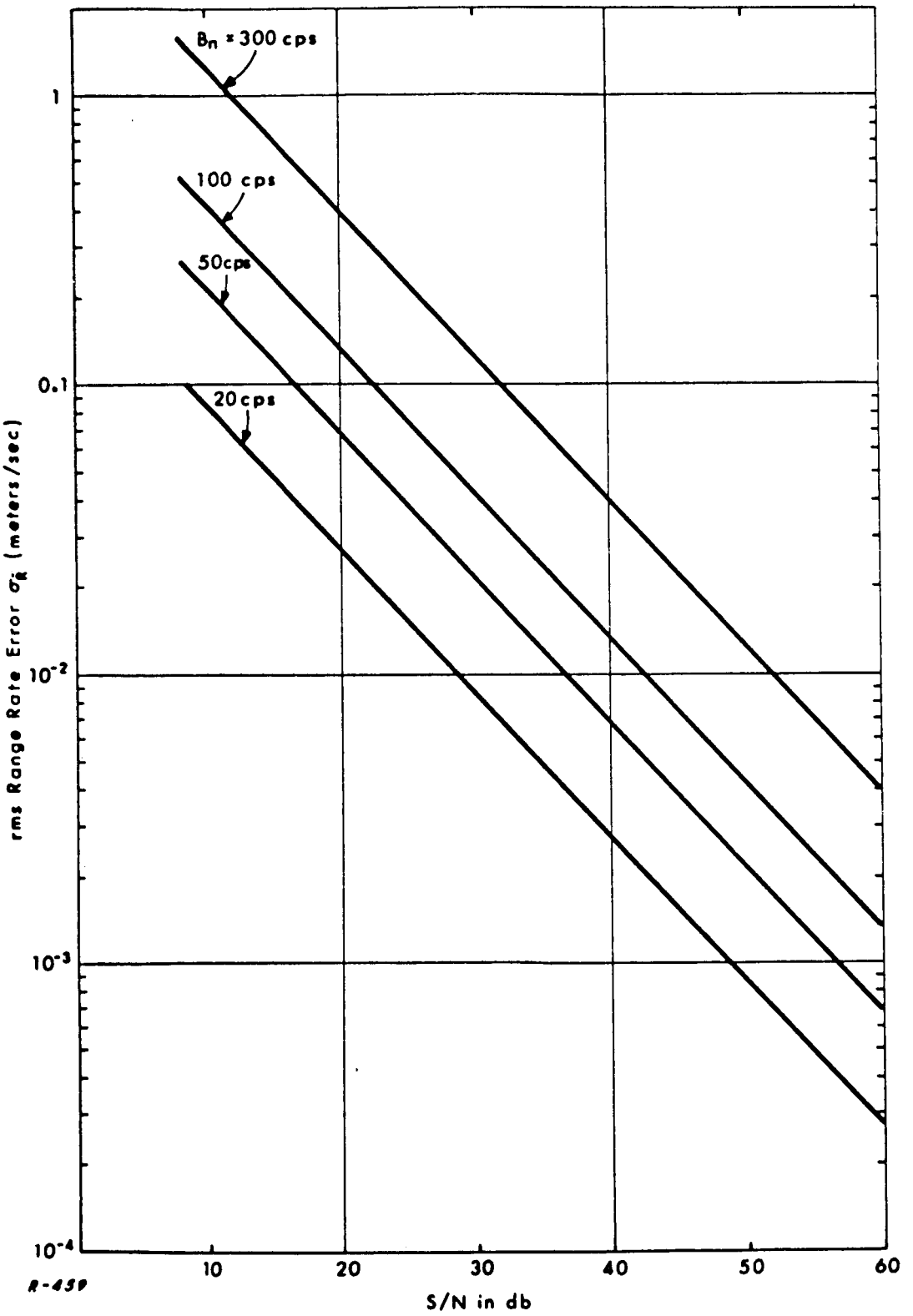

Fig. 8 Plots of rms range-rate error $\sigma_{\dot{R}}$ as a function of S/N ratio in carrier isolation bandwidth B_n, for various values of B_n, and for S-Band system design parameters.

5. Performance of Operating GRARR Systems

The Goddard Range and Range Rate System has thus far been used successfully on four spacecraft missions. They were the Interplanetary Monitoring Platforms (IMP) A, B and C and the Eccentric Orbiting Geophysical Observatory (EOGO or EGO) A. The three IMP missions utilized the VHF system while the EGO utilized the S-Band system.

The IMP missions have provided a considerable quantity of data that have been used to check system performance. The EGO mission, while proving S-Band performance, has been hampered by the fact that the attitude control system of the spacecraft was not able to provide the proper orientation, and so the R + R transponder antenna was not facing the earth as planned. This has resulted directly from the failure of some of the spacecraft booms to deploy. Consequently, data were obtainable only over a small portion of the orbit.

IMP A achieved an orbit with an apogee of approximately 200,000 km and a perigee of approximately 300 km. The transponder was modified so that, in the ranging mode, the power in the sidebands was shared equally with the telemetry signal. With 0.5 rad of phase deviation assigned to the ranging tones and 0.5 rad assigned to telemetry, the distribution of signal power in the resulting downlink spectrum, relative to the unmodulated carrier, was as follows:

carrier	- 1.1 db
subcarrier	-11.5 db
20 kc tone	-17.2 db
other tones	-28.7 db

On this basis the power balance figures are as given in Table IV. Reference to this table shows that in the IMP A mission the subcarrier thresholds were reached at apogee. Consequently, data were not always obtainable.

In IMP B, the power was distributed on the basis of 0.7 rad of carrier phase deviation for ranging and 0.2 rad for telemetry. IMP B, however, did not reach the apogee of IMP A and hence the threshold condition was

Table IV

Link Power Figures for IMP A

	carrier	subcarrier	20 kc tone
Spacecraft power out	+ 34.9 dbm	24.5 dbm	+ 18.8 dbm
Space loss (200,000 km)	-181 db	-181 db	-181 db
Antenna gain spacecraft	- 4 db	- 4 db	- 4 db
Antenna gain ground	+ 19 db	+ 19 db	+ 19 db
Miscellaneous losses	- 6 db	- 6 db	- 6 db
Received signal power	-137.1 dbm	-147.5 dbm	-153.2 dbm
Noise figure (plus preselector)	+ 4 db	+ 4 db	+ 4 db
Sky noise (additional)	+ 3 db	+ 3 db	+ 3 db
Receiver noise density	-167 dbm/cps	-167 dbm/cps	-167 dbm/cps
Receiver bandwidth ($2\beta_L$)	20 cps	10 cps	0.1 cps
Received S/N ratio	+ 16.9 db	+ 9.5 db	+ 23.8 db

never reached. IMP C used the same power distribution as IMP B and good data have been obtained at an apogee of approximately 250,000 km.

The data from IMP A have been analyzed and compared with the expected results as a function of range. These results are shown in Figs. 9 and 10.

Acknowledgment

The conception, design and evolution of the GRARR system are the result of a team effort combining several organizations. Under the leadership of members of the Network Engineering Branch of Goddard Space Flight Center, assisted by ADCOM, Inc. under Contract NAS 5-1187, the system has evolved from a set of requirements to the current operating and projected round-the-world stations constructed by Motorola, Inc., and General Electric Company. Among the individuals who have made outstanding contributions are E.J. Habib, P.D. Engels and H.W. Shaffer of NASA GSFC and K.W. Kruse of ADCOM, Inc. The authors are gratefully indebted to these dedicated colleagues for invaluable support and discussions in the generation of this paper.

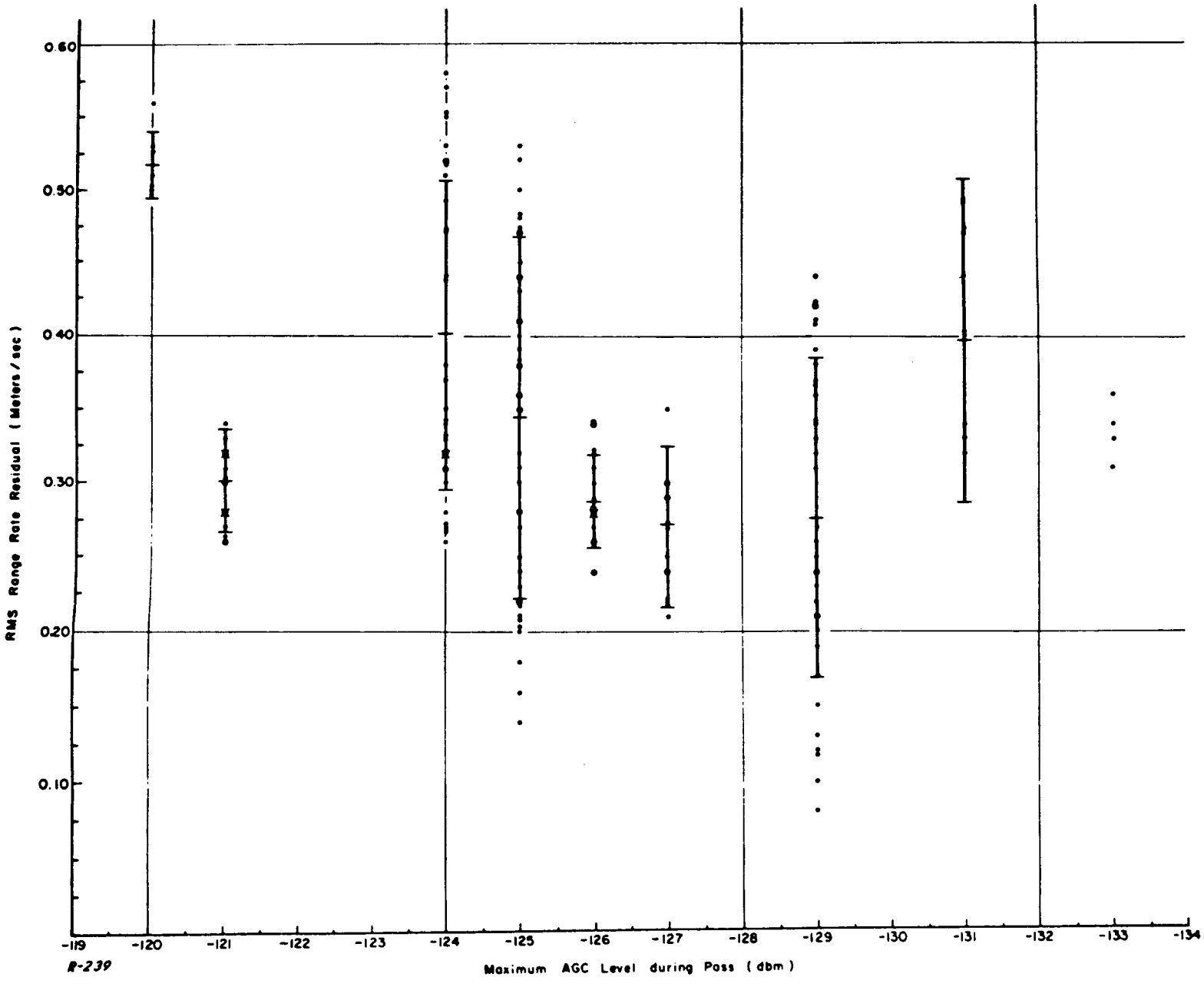

Fig. 9 Standard deviation of range-rate measurements observed from IMP-A (design goal = 1.0 m/sec).

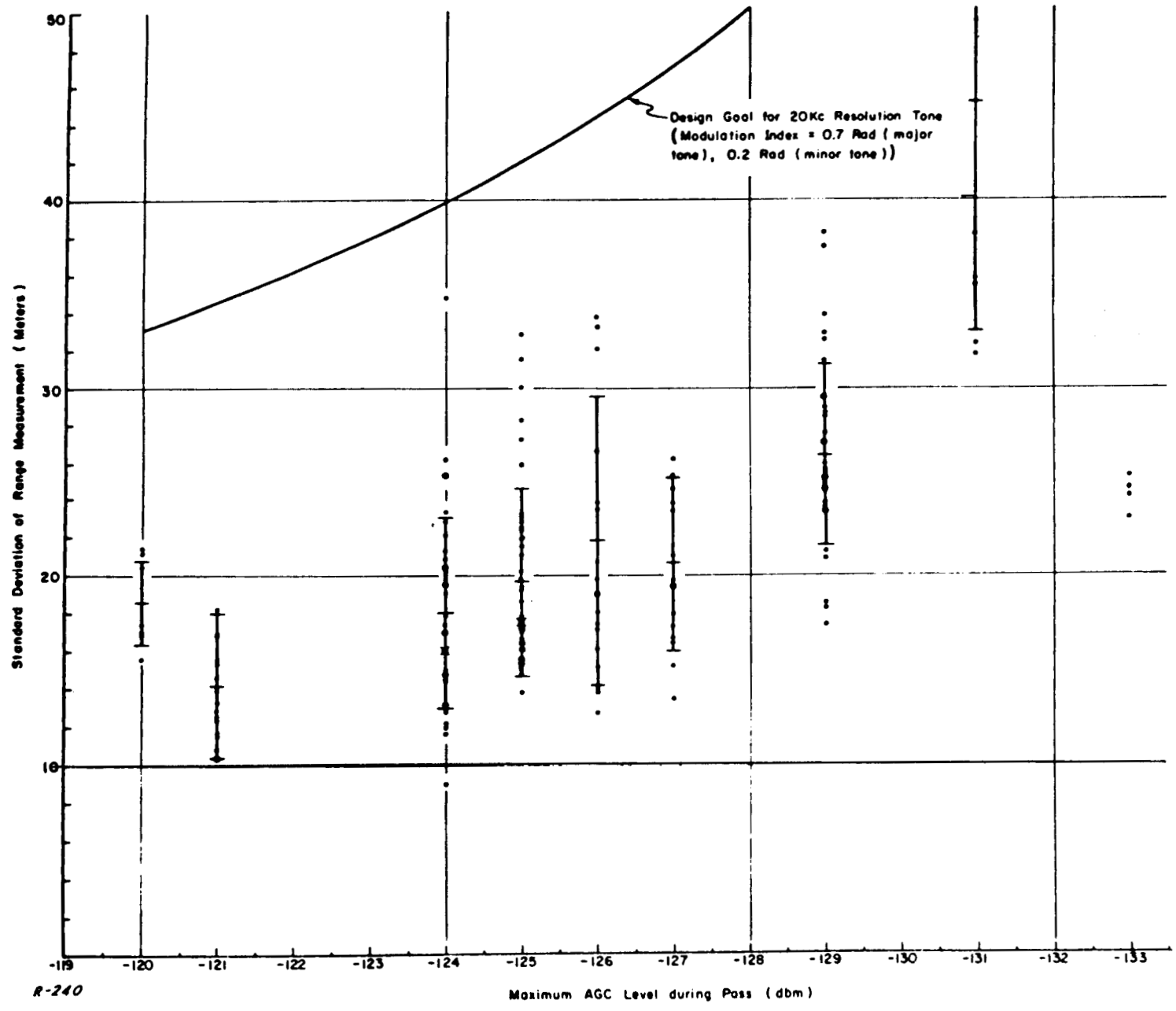

Fig. 10 Standard deviation of range measurements observed from IMP-A.

REFERENCES

1. E. J. Habib, G. C. Kronmiller, Jr., P. D. Engels, and H. J. Franks, Jr., Development of a Range and Range Rate Spacecraft Tracking System, NASA Tech. Note NASA TND-2093; Goddard Space Flight Center, Greenbelt, Maryland, June 1964. (Originally published in 1961 as a NASA internal document.)

2. E. J. Baghdady and K. W. Kruse, "The Design of Signals for Space Communications and Tracking," 1964 IEEE International Convention Record, Part 7, pp. 152-174; March, 1964.

3. L. D. Baumert, M. F. Easterling, S. W. Golomb and A. J. Viterbi, Coding Theory and its Applications to Communications Systems, Tech Report No. 32-67, Jet Propulsion Laboratory, Pasadena, Calif., March, 1961.

4. E. J. Baghdady, Lectures on Communication System Theory, McGraw-Hill Book Co., New York, 1961; Chapter 19.

5. R. T. Fitzgerald, P. D. Engels, H. W. Shaffer, E. J. Habib and M. J. Mitchko, A Hybrid Ranging System for Spacecraft, NASA Document X-531-64-71, Goddard Space Flight Center, Greenbelt, Maryland; April, 1964.

6. JPL Space Programs Summary No. 37-21, Vol. III, Jet Propulsion Laboratory, Pasadena, Calif.; May 31, 1963.

7. ADCOM, Inc., High-Accuracy Satellite Tracking Systems, Third Quarterly Report, Contract No. NAS 5-1187; December 31, 1961.

8. E. J. Baghdady, "On the Noise Threshold of Conventional FM and PM Demodulators," Proc. IEEE, Vol. 51, pp. 1260-1261; September, 1963.